HHS Public Access

Author manuscript

Small. Author manuscript; available in PMC 2016 September 16.

Published in final edited form as:

Small. 2015 September 16; 11(35): 4423–4444. doi:10.1002/smll.201500970.

Plasmofluidics: Merging Light and Fluids at the Micro-/Nano-Scale

Mingsong Wang,
Department of Mechanical Engineering, Materials Science and Engineering Program Texas Materials Institute The University of Texas at Austin, Austin, Texas 78712, USA

Prof. Chenglong Zhao,
Department of Physics Electro-Optics, Graduate Program University of Dayton, Dayton, Ohio 45469, USA

Dr. Xiaoyu Miao,
Google, Inc., 1600 Amphitheatre Pkwy, Mountain View, CA 94043, USA

Yanhui Zhao,
Department of Engineering Science and Mechanics, Department of Biomedical Engineering, Materials Research Institute, Huck Institute of Life Sciences, The Pennsylvania State University, University Park, Pennsylvania 16802, USA

Joseph Rufo,
Department of Engineering Science and Mechanics, Department of Biomedical Engineering, Materials Research Institute, Huck Institute of Life Sciences, The Pennsylvania State University, University Park, Pennsylvania 16802, USA

Dr. Yan Jun Liu,
Institute of Materials Research and Engineering, Agency for Science, Technology and Research (A*STAR) 3 Research Link, Singapore 117602, Singapore

Prof. Tony Jun Huang, and
Department of Engineering Science and Mechanics, Department of Biomedical Engineering, Materials Research Institute, Huck Institute of Life Sciences, The Pennsylvania State University, University Park, Pennsylvania 16802, USA

Prof. Yuebing Zheng
Department of Mechanical Engineering, Materials Science and Engineering Program Texas Materials Institute The University of Texas at Austin, Austin, Texas 78712, USA

Yan Jun Liu: liuy@imre.a-star.edu.sg; Tony Jun Huang: junhuang@psu.edu; Yuebing Zheng: zheng@austin.utexas.edu

Abstract

Plasmofluidics is the synergistic integration of plasmonics and micro/nano fluidics in devices and applications in order to enhance performance. There has been significant progress in the emerging field of plasmofluidics in recent years. By utilizing the capability of plasmonics to manipulate

Correspondence to: Yan Jun Liu, liuy@imre.a-star.edu.sg; Tony Jun Huang, junhuang@psu.edu; Yuebing Zheng, zheng@austin.utexas.edu.

light at the nanoscale, combined with the unique optical properties of fluids, and precise manipulation via micro/nano fluidics, plasmofluidic technologies enable innovations in lab-on-a-chip systems, reconfigurable photonic devices, optical sensing, imaging, and spectroscopy. In this review article, we examine and categorize the most recent advances in plasmofluidics into plasmon-enhanced functionalities in microfluidics and microfluidics-enhanced plasmonic devices. The former focuses on plasmonic manipulations of fluids, bubbles, particles, biological cells, and molecules at the micro-/nano-scale. The latter includes technological advances that apply microfluidic principles to enable reconfigurable plasmonic devices and performance-enhanced plasmonic sensors. We conclude with our perspectives on the upcoming challenges, opportunities, and the possible future directions of the emerging field of plasmofluidics.

1. Introduction

Plasmonics is a field dedicated to the fundamental study and applications of surface plasmons (SPs), which are the light-coupled coherent oscillations of free electrons at the interfaces of metals and dielectric materials.[1–3] The ability of SPs to manipulate light at the nanoscale leads to numerous intriguing physical phenomena such as localized heating[4,5] and plasmon-induced transparency.[6–8] Although the underlying mechanisms are quite simple, plasmonic structures and devices can have broad applications[9–12] and have been employed to solve many challenges that arise due to the diffraction limit of conventional optics. For example, surface plasmon resonance (SPR) sensors, which utilize the critical excitation conditions of surface plasmon waves to detect molecular-scale interactions on metal surfaces, have been successfully commercialized and have become an essential tool for characterizing and quantifying biomolecular interactions.[13–15] Other notable inventions in the field of plasmonics include “invisibility cloaking” materials that do not exist in nature[16,17] and small “satellites” that have been used to investigate organelle structures inside of single cells.[18,19]

The fusion of plasmonics and micro/nano fluidics is by no means accidental and offers exciting opportunities to advance both fields. Each field possesses inherent strengths and advantages that the other generally lacks. Plasmonic devices are capable of detecting chemical changes and binding events with single molecule resolution, but lack a means of precisely delivering an analyte sample in a high-throughput manner.[20,21] In contrast, micro/nano fluidic devices are capable of precise, high-throughput delivery of fluids, but lack the ability to simultaneously perform highly sensitive measurements. These problems can be solved by a “plasmofluidic” approach, which leverages the strengths and advantages of plasmonics and micro/nano fluidics. Since the integration of plasmonics with nanofluidics is an emerging frontier that has only begun to be explored, in this review article, we will focus on the integration of plasmonics and microfluidics. By analyzing recent trends in the fields of plasmonics and microfluidics, it can be seen that the crossover between the two fields has already started. Some plasmonic effects, such as the propagating surface plasmon polaritons (SPPs) and localized surface plasmon resonances (LSPRs), have already led to commercialized SPR sensors and microfluidic surface-enhanced Raman spectroscopy (SERS) for the clinical detection and diagnosis of numerous solution-based analytes.[22]

The success of “optofluidics”, which synergistically combines microfluidics with optics, sets an excellent precedent for the development of “plasmofluidics”.[23–31] With major efforts towards developing miniaturized on-chip imaging systems and fluidic devices that manipulate light at the microscale, optofluidics broke down the barrier between microfluidics and conventional optics, making it possible for the invention of devices and systems such as “on-chip flow cytometers”[32,33] and “cellphone microscopes”.[34,35] With its ability to extend conventional optics into nanoscale regimes, “plasmofluidics” provides excellent opportunities for exploring new physical phenomena as well as enabling novel applications such as “plasmofluidic lenses”[36] and single-molecule detection platforms enabled by “plasmofluidic chips”.[37] In this review article, we will share with you some of the most important works in this emerging field. We envision that plasmofluidics will push the boundaries of traditional engineering approaches and bridge the two research fields of plasmonics and microfluidics. With much yet to be explored, we hope that the recent advances outlined in this review article will inspire others in these fields to take innovative steps to explore novel plasmofluidics combinations that can have a lasting impact on the world.

2. Plasmon-Enhanced Functionalities in Microfluidics

Due to the unique optical, mechanical, and thermal properties at the nanoscale, surface plasmons can enhance various functionalities related to the manipulation of fluids, bubbles, particles, cells, and molecules in microfluidics. Precise manipulations of fluids and biomaterials are essential to immunoassays, cell-molecule interaction studies, DNA hybridization, catalysis, and drug delivery.[20,21,38,39] Light is an ideal energy source since it can be controlled remotely and easily integrated with a variety of platforms via readily available optical components. For example, optical tweezers employ focused laser beams to provide mechanical forces that can be used to precisely manipulate single cells, cellular organelles, or biomolecules with high spatial resolution.[40] After roughly three decades of evolution, using light to trap and manipulate single particles in microfluidic environments has become a gold-standard approach in biophysics and cell biology.[41–43] However, it remains a significant challenge to focus light beyond the diffraction limit in order to generate enough gradient force to trap nanoparticles and biomolecules. As described in the following sub-sections, SPs offer an excellent solution to enhancing the trapping ability of particles and biomaterials at the nanoscale. Moreover, the photothermal effects associated with the local plasmonic losses provide a unique way for low-power and long-range manipulation of fluids and bubbles.[44–59]

2.1. Plasmonic Manipulation of Fluids and Bubbles

Enhanced photothermal effects are associated with the non-radiative decay of SPs on metal nanostructures. They arise from the energy relaxation of coherently oscillated electrons upon their interaction with the metal lattice after the excitation of SPs.[60,61] In metal nanoparticles, the heat induced by LSPRs is highly localized.[60,62] Such highly localized heat sources have enabled the optical manipulation of both microscale fluids and bubbles in fluids without the need for complex valves and pumps. Here we discuss three types of plasmonic manipulations, *i.e.*, control of fluid flow, fluid mixing, and bubble generation.

Controlling Fluid Flow—Liu *et al.* presented a seminal work on using the plasmon-enhanced photothermal effects of metal nanoparticles to control fluid flow (Figure 1).[44] Metal nanoparticles dispersed in fluids act as localized thermal sources upon excitation of SPs and cause the fluids to evaporate. The condensation of vapors into droplets and their coalescence with the original fluids result in a net movement of the fluids. Using light beams with sub-milliwatt power, fluid flow in microfluidic channels can be directed remotely at controlled speeds and directions. Due to the nanoscale localization of thermal energy, most of the fluid remains at room temperature, making this method of fluid transportation suitable for many biological applications.

To further improve the plasmon-enhanced photothermal effects for fluid manipulation, metal nanoparticles can be incorporated into microfluidic channels. For example, Fang *et al.* have developed poly(dimethylsiloxane) (PDMS) channels embedded with Au nanoparticles. A T-shaped microfluidic channel made of the nanoparticle/PDMS composites was fabricated to demonstrate the optical control of flow of thermoreversible gelation polymer, known as thermorheological fluid (Figure 2).[46]

Advanced flow control for the separation and distillation of microscale liquids has been achieved by combining LSPR-enhanced photothermal effects with bubble-assisted interphase mass-transfer.[45] As shown in Figure 3, a gas bubble is generated and captured in the fluid via plasmon-enhanced photothermal effects on a substrate that is coated with metal nanoparticles and covered with PDMS microfluidic channels. The separation process occurs when a laser beam focused on one edge of the bubble evaporates the fluid and the vapor condenses on the other side of the bubble.

In addition to versatile applications in lab-on-a-chip systems, plasmon-enhanced photothermal control of fluid flow has also enabled photoswitchable electrical devices. For example, Xia and coworkers have demonstrated that plasmonic heating can be used to control fluid flow, which in turn can enable the reversible photoswitching of a light-emitting diode (LED).[47] As shown in Figure 4, the fluid-flow-based switch was constructed from a small vial connected to a capillary containing two standard copper wires with a gap of 5 mm between their ends. A conductive aqueous suspension of Au nanoparticles saturated with NaCl was used as the fluidic medium. Upon irradiation with a laser beam at the LSPRs of metal nanoparticles, the solution was heated up and expanded along the capillary due to the photothermal effects. The expansion bridged the gap between the two wires and completed an electrical circuit, which turned on the LED. When the laser was off, the solution level dropped and the LED was switched off.

Mixing Fluids—Mixing of fluids is another critical function in microfluidics and lab-on-a-chip devices. Conventional light-induced microfluidic mixing requires high-intensity light sources (7.6×10^{10} W/cm^2). Such high-intensity light may exceed the safety threshold of living tissues in bio/medical applications, which can cause some undesirable side effects, such as photodamage.[63] Miao *et al.* have demonstrated that the LSPR-assisted photothermal effects enable microfluidic mixing at low optical power.[48] By employing Au nanoparticle arrays on substrates, light with intensity as low as 6.4×10^{3} W/cm^2 has been used to generate the efficient convective flow for fluid mixing (Figure 5). This ~7 orders of

magnitude reduction in the input light intensity makes the light-based mixing process biocompatible.

Generating Bubbles—Bubbles in fluids have attracted significant efforts in research communities because of their potential applications in particle manipulation, drug delivery, and cancer therapy.[49–55] Plasmonic-enhanced photothermal effects have been applied to generate and manipulate bubbles in various environments for different applications. Lapotko and co-workers used plasmon-assisted bubble generation inside a liposome to release molecules at a specified site for targeted drug delivery (Figures 6a–c).[56] In another application, by generating bubbles in fluids through a tapered optical fiber decorated with Au nanorods, Li *et al.* realized effective trapping and aggregation of microparticles at a desired location (Figures 6d–f).[57]

2.2. Plasmonic Manipulation of Particles, Cells, and Molecules in Fluids

The ability to manipulate particles, cells, and molecules in fluids is another critical function in microfluidic systems and lab-on-a-chip devices. Optical tweezers have provided researchers with a simple, noninvasive, yet effective method to manipulate particles, cells and molecules in fluids. However, conventional optical tweezers have several limitations, including bulky and expensive equipment, ineffective manipulation of nanoparticles due to the significantly reduced trapping force with the diffraction-limited laser spots, and the use of high-power lasers that may potentially damage cells and living organisms. Due to the increased trapping force associated with the sub-wavelength localization of the near-field SPs, plasmonic tweezers are ideal for manipulating sub-wavelength objects with low laser power. Moreover, the two-dimensional (2D) nature of SPs facilitates their on-chip integration. Recent years have witnessed tremendous progress in plasmonic tweezers for micro-/nano-scale trapping and three-dimensional (3D) manipulation of cells and nanoparticles.

Trapping Microparticles with SPPs—Volpe *et al.* reported the experimental observation of momentum transfer from SPPs to a single particle, revealing the potential for plasmonic manipulations.[64] In their study, the strong SPP field excited on a homogeneous Au film generates an optical force 40 times stronger than that at the absence of plasmonic excitation and hence significantly decreases the laser power for particle manipulations. Later, Garcés-Chávez *et al.* demonstrated the large-scale aggregation of colloidal microparticles based on SPs on an Au thin film.[65] They have shown that the controlled excitation of SPPs permits the use of combined optical and thermal forces for large-scale ordering of colloidal aggregations. In order to use SPs to trap single microparticles, Righini *et al.* patterned the continuous Au thin film into microscale pads. Each pad restricts the SPs into a smaller regime with the modified optical potential for the effective trapping and even sorting of single microparticles of a specific size.[66]

Trapping Nanoparticles with LSPRs—An effective way of trapping nanoparticles is the use of plasmonic nanoantennas, which are paired metal nanostructures with small gaps between them that support highly confined LSPRs. The high confinement of light at the gaps provides a strong gradient force for trapping.[67,68] Grigorenko *et al.* demonstrated the

trapping of nanoparticles based on the paired Au nanodots on a substrate.[67] With the enhancement of the optical field at the antennas, reduced exciting light intensities for trapping have been reported for different particles and bacteria (*e.g.*, 10^7 W/m^2 for polystyrene beads and ~10^8 W/m^2 for *Escherichia coli* bacteria).[68] For comparison, to trap Escherichia coli with conventional optical tweezers typically requires an exciting laser intensity greater than 10^9 W/m^2, and previous report has shown that significant damage occurs to the Escherichia coli at a light intensity of ~10^{10} W/m^2.[69] So far, plasmonic nanoantennas have been designed to trap Au colloids and quantum dots down to 10 nm.[70,71] The capability of trapping nanoparticles within small gaps has also significantly benefited plasmon-enhanced optical spectroscopy, including SERS.[72,73] By combining plasmonic trapping with light-assisted molecular immobilization, Galloway *et al.* precisely trapped Au nanocolloids within “hot spots” of the antennas for the ultrahigh-sensitive spectroscopy (Figure 7).[73]

Despite the significant progress in using SPs to trap and manipulate ever-smaller objects, stably trapping sub-10 nm particles has remained a challenge. Recently, Saleh *et al.* demonstrated theoretically that coaxial plasmonic apertures have the potential to trap dielectric particles as small as 2 nm in both air and water (Figure 8). The coaxial apertures benefit from the extremely confined light at such small volumes. Such plasmonic nanostructures can lead to the on-chip trapping of single nanoscale airborne particles in aerosols and single small molecules in microfluids.[74]

Trapping Nanoparticles with Self-Induced Back Action—To further reduce the power of trapping light, self-induced back action (SIBA) plasmonic trapping has been developed.[75] SIBA is based on the interaction between metal apertures and the trapped dielectric particles. Briefly, when a particle with a refractive index larger than that of the surroundings is trapped in a metal aperture, the aperture ‘appears’ larger and allows the enhanced transmission of light. When the trapped particle is moved out of the aperture, light transmission will drop, which is related to a drop in the rate of photon momentum traveling through the aperture. As a result, a force in the opposite direction will act on the particle to balance this momentum rate change and pull the particle back to the equilibrium position, *i.e.*, the inside of the aperture. Because particles play such an active role, SIBA optical trapping can use low light intensities.

Following the initial demonstration of SIBA optical trapping of nanoparticles based on nanoapertures in metal thin films by Juan *et al.*,[75] Chen *et al.* applied SIBA to successfully trap single or double 22 nm polystyrene beads.[76] Gordon and co-workers employed double-nanoholes on an Au thin film to trap dielectric nanoparticles with diameters down to 12 nm with a reduced light intensity.[77] Recently, using the same plasmonic substrates, the Gordon group has successfully trapped a single protein and protein-antibody pairs.[78–81]

Beyond the static trapping, the 3D manipulation of sub-100 nm dielectric objects has also been achieved with SIBA.[82] Using an optical fiber probe with a bowtie nano-aperture at the tip for the SIBA-based trapping, Quidant and co-workers have successfully trapped and manipulated sub-100 nm dielectric objects in 3D within a microfluidic chamber (Figure 9).

The manipulation allows the trapped objects to be moved over tens of micrometers over a period of several minutes with low light intensities.

Developing Plasmonic Tweezers Based on Multiple Types of Forces—So far, we have focused on particle trapping and manipulation with the radiation force arising from SPs in fluidic environments. By balancing the radiation force, thermal convection, and thermophoresis, researchers have expanded the capabilities of plasmonic tweezers. Along this line, Roxworthy *et al.* have achieved the trapping, sorting, and clustering of microparticles based on Au bowtie nanoantennas by controlling multiple parameters, including light intensity, wavelength, and polarization.[83] In another example, Shoji *et al.* demonstrated the manipulation of fluorescent polystyrene nanospheres based on arrays of Au nanopyramidal dimers. Using fluorescence microscopy to visualize the motion of nanospheres, they have verified that thermal convection plays a critical role in the nanosphere transportation (Figure 10).[84] Recently, Toussaint and co-workers have developed an array of plasmonic nanoantennas on indium-tin-oxide (ITO) substrates to increase the thermal fluid convection from conventional nanometers per second to micrometers per second for the enhanced performance in nanoparticle manipulation and assembling.[85]

Reducing Negative Thermal Effects in Plasmonic Tweezers—Despite its use in the manipulation of fluids and particles, plasmon-enhanced photothermal energy can potentially cause trapping instability and damage to the trapped organisms. To reduce the negative impact of thermal energy, researchers have developed several approaches, including the use of heat sinks, optical vortices, and low-power ultrafast light sources. Wang *et al.* integrated heat sinks with plasmonic nanostructures to reduce the undesired thermal effects.[86] By using a three-layer (Au, Cu, and Si) stack of high-thermal-conductivity materials as a substrate, they have significantly reduced water heating and succeeded in trapping and rotating nanoparticles via control of incident light polarization. Kang *et al.* developed an optical vortex trapping with a diabolo nanoantenna.[87] In contrast to a conventional light beam, the optical vortex can trap specimens at regimes away from the hot spots, significantly reducing the potential thermal damages to the trapped specimens. Roxworthy *et al.* demonstrated that plasmonic tweezers using a femtosecond-pulsed light source could work at the ultra-low power density of 20 mW/mm^2, a power level approximately 3 orders of magnitude lower than the optical damage threshold.[88] Later, Shoji *et al.* employed the femtosecond-pulsed plasmonic tweezers to realize the reversible trapping and releasing of DNAs.[89]

Achieving Simultaneous Manipulation, Monitoring, and Analysis—The ability to monitor manipulation events and measure trapped specimens is essential for achieving real-time sensing and feedback with tweezers. Due to the sensitivity of SPs to the surroundings and the plasmon-enhanced optical spectroscopy, plasmonic tweezers have been developed to achieve simultaneous manipulation, monitoring, and analysis. For example, Martin and co-workers have achieved the simultaneous trapping and sensing of 10 nm particles with plasmonic nanoantennas.[70,90] Based on the sensitivity of light transmission through the

nanoapertures to the movement of nanoparticles, SIBA-based plasmonic tweezers have also enabled simultaneous trapping and sensing.[75–80,91]

Exploiting Multiple Beams of SPPs—In order to develop more advanced trapping capabilities and improved overall functionality, researchers have worked beyond single propagating SPPs to demonstrate the trapping, propelling, and sorting of small particles based on two or more SPPs. For example, Wang *et al.* irradiated Au strips with two laser beams of the same wavelength from opposite directions to create the interference patterns of SPPs for the trapping and propelling of polystyrene particles.[92] Optical sorting of Au nanoparticles of two different sizes in fluids was accomplished by applying two counter-propagating evanescent waves of different wavelengths at the fluid-substrate interface (Figure 11).[93] This strategy is applicable to the plasmonic sorting with an improved efficiency by coating the substrate with an Au thin film.

Recently, Min *et al.* have demonstrated highly focused SPP fields on an Au thin film through constructive interference of multiple SPPs, which enables the trapping of single metal particles without the need to pattern substrates – a requirement for the use of conventional single SPPs.[94] The focused SPP fields, which are excited by a radially polarized beam using a microscope with high numerical aperture objectives, trap metal particles with both gradient and scattering forces acting in the same direction (Figure 12).[94] Controlling the position of the microscope objective enables the versatile 2D manipulation of the trapped particles.

In summary, the unique optical, mechanical, and thermal properties of SPs open up a new window of opportunities for versatile manipulations of both fluids in micro-/nano-scale channels and bubbles, particles and biomaterials in fluidic environments. Progress in nanofabrication, characterization, and simulations has allowed for a broad range of manipulations at different scales (microscale and nanoscale) and dimensions (2D and 3D). Some of these manipulation techniques are readily integrated with microfluidic systems for the enhanced functionalities in lab-on-a-chip devices. Others require the coordinated efforts in system design and integration in order to achieve the synergy of plasmonic manipulations and microfluidics.

3. Microfluidics-Enhanced Plasmonic Devices

The unique optical properties of fluids and the versatile manipulation of fluids via microfluidic technology have provided great opportunities for enhanced or new functionalities in a broad range of plasmonic devices such as plasmonic circuits,[95–97] planar lenses,[98–101] metamaterials,[102,103] and super-resolution imaging.[104–107] By combining SPs with microfluidic devices that can manipulate liquids of different optical properties or modify the shape of liquid-metal interfaces, a new class of reconfigurable plasmofluidic devices has been demonstrated.[36,108–126] The microfluidics-enhanced reconfigurable devices offer a much broader tuning range of SPs than the traditional approaches that are based on the tunable properties of solid-state dielectric materials or metal structures.[127–131] Another major plasmonic application that has significantly benefited from microfluidics are plasmonic sensors. Through the precise delivery and

manipulation of analyte solutions and metal nanoparticles, microfluidic technology has greatly enhanced throughput and sensitivity of various types of plasmonic sensors.[132–140] It is expected that the synergy of plasmonic sensors and microfluidics will enable fully integrated, portable, and cost-effective diagnostic devices that will greatly benefit global healthcare. In the following sub-sections, we will discuss the microfluidics-enhanced plasmonic devices in two categories, *i.e.*, reconfigurable plasmonic devices and plasmofluidic sensors.

3.1. Reconfigurable Plasmonic Devices

Reconfigurable plasmonic devices in which the SPs are actively modulated with external signals are important for many applications such as information technology and energy conversions. SPs at a dielectric-metal interface can be modulated by controlling the optical properties of the dielectric material and/or metal. Many functional dielectric materials have been demonstrated for the active tuning of SPs, including thermal-optical polymers[127] and electro-optic materials.[128,129] Ultrafast optical pumping of metals[130] and controlled semiconductor-metal phase transitions have also led to reconfigurable plasmonic devices.[131] However, the tunable range (or modulation depth) of SPs based on the solid-state materials is limited by the small changes in their optical properties.

Among various strategies for the enhanced tunability of SPs, the use of fluids or fluid-solid phase transitions in plasmonic devices has attracted strong interests. Compared with solid-state materials, fluids have three intrinsic characteristics that enable precise and broadband tunability in plasmonic devices: high mobility, reconfigurability, and a large range of refractive indices. So far, various reconfigurable plasmofluidic devices that employ fluidics for active control of SPs have been developed. Herein, we structure these devices into three categories based on the control mechanisms, *i.e.*, tuning the optical properties of fluids surrounding metals, controlling liquid-solid phase transitions of metals, and controlling the arrangements of metal nanoparticles at the interfaces of fluids.

Tuning the Optical Properties of Fluids Surrounding Metals—Various approaches have been developed to modulate the optical properties of fluids to achieve the active control of SPs for reconfigurable plasmonic devices, including bubble generation in fluids and phase transition in liquid crystals. Zhao *et al.* demonstrated a “plasmofluidic lens”, which enables the active control of SPs on a 2D plane based on the on-demand generation of vapor bubbles in fluids.[36] As shown in Figure 13a, an Au thin film acts as both an SP substrate and an effective heating base for the bubble generation. SPs are generated and focused by an arc grating structure. Controlling surface bubbles in terms of their positions and shapes has led to dynamic tuning of the focusing function of the lens due to the modulations of the refractive index of the surroundings at the plasmonic substrate (Figure 13b–e). To realize dynamic modulation of out-of-plane light, Wang *et al.* demonstrated a reconfigurable plasmonic device based on the extraordinary optical transmission (EOT) of bullseye structures and the flow control of eutectic gallium indium (EGaIn), a liquid metal.[108,141] EGaIn has been reversibly injected into or withdrawn from a microfluidic channel on top of the bullseye structures to dynamically modulate SPs and EOT.

Reconfigurable plasmofluidic devices have also been realized by controlling LSPRs of metal nanoparticles with fluids surrounding the nanoparticles. Fang *et al.* have demonstrated that the dynamic control of a vapor nanobubble around an Au nanoparticle actively tunes the LSPRs.[109] As shown in Figure 14a, illuminating the nanoparticle with a continuous-wave laser beam of sufficient intensity generates the nanobubble that originates from boiling the liquid at a single nanoparticle nucleation site. The nanobubble generation caused a blue shift in the LSPRs of the Au nanoparticle due to the reduced refractive index of the surroundings (Figure 14). Lapotko and co-workers have also used pulsed laser to generate transient vapor nanobubbles around metal nanoparticles to tune the LSPRs in an ultrafast fashion.[56,110,111]

Liquid crystals are functional fluids that have found broad application in reconfigurable photonic and plasmofluidic devices.[142] Liquid crystals possess the largest birefringence among all known materials and the birefringence spans the visible-infrared spectrum and beyond. The phase of liquid crystals can be controlled by various signals such as electricity,[143,144] light,[145–147] and acoustic waves.[148] So far, various active plasmonic devices based on liquid crystals have been developed, including switches[112–114,149] and modulators.[115–118] For example, Liu *et al.* demonstrated light-driven plasmonic color filters by covering the metal annular aperture arrays on substrates with photoresponsive liquid crystals (Figure 15a).[119] Doping liquid crystals with azobenzene molecules, which undergo reversible *trans-cis* photoisomerization, enables optical control of the phase of liquid crystals. As shown in Figure 15b, color filters with different aperture sizes have been designed to allow different regimes of working wavelengths. The all-optical tuning behavior of the color filters has been highly reversible. In another example, as demonstrated by Smalyukh and co-workers, plasmonic nanostructures can also be dispersed within the liquid crystals where an external field realigns the liquid crystal matrix to switch the LSPRs.[120,121,150]

Controlling Liquid-Solid Phase Transitions of Metals—The solid-liquid phase transition in metals has provided another route towards the reconfigurable plasmonic devices based on the difference in the optical properties of metals in different phases. For example, Krasavin and Zheludev employed a Ga solid-liquid phase transition to modulate SPPs in a metal-on-dielectric plasmonic waveguide.[151] Odom and co-workers reported a tunable 1D Ga grating. The grating exhibits temperature-dependent plasmonic properties due to the solid-liquid phase transition of Ga (Figure 16).[122] The plasmonic properties of the Ga gratings can be switched by thermally inducing solid-to-liquid and liquid-to-solid phase transitions. The switching is highly reversible throughout extensive cycling.

Controlling the Arrangement of Metal Nanoparticles at the Interfaces of Fluids —Due to its self-healing, non-degrading, and renewable properties, the interfaces of different fluids provide an ideal platform for the formation of 2D monolayers of metal nanoparticles. Active tuning of the structure and coverage of the monolayers paves another way towards reconfigurable plasmofluidic devices due to the sensitivity of SPs to the distance-dependent couplings among the nanoparticles within the monolayers.[123–125] For instance, Fang *et al.* demonstrated a dynamic mirror made of 60 nm Au nanoparticles assembled as a monolayer at a [heptane + 1,2-dichloroethane]/water liquid/liquid

interface.[126] Figure 17a shows that a green laser light (λ = 532 nm) is reflected at the Au nanoparticle mirror with concurrent absorption and scattering. The reflectivity of the mirror can be tuned by changing the surface coverage of the Au nanoparticles (Figure 17b).

3.2. Plasmofluidic Sensors

Due to the plasmon-enhanced light-matter interactions at the nanoscale, plasmonic sensors enable sensitive detection of chemical and biological analytes. These nanoscale optical sensors have been explored for applications in medical diagnostics,[152–154] food control,[155–157] and environmental monitoring.[158,159] With the versatile manipulations of fluids, nanoparticles, and analytes, microfluidics has significantly enhanced the sensitivity and throughput of plasmonic sensors. Various plasmofluidic sensors that merge microfluidics and plasmonic sensors are emerging, which can be categorized into plasmonic spectroscopy and surface-enhanced Raman spectroscopy.

3.2.1 Plasmonic Spectroscopy—Plasmonic spectroscopy detects analytes by measuring the analyte-induced changes in the optical transmission/absorption/reflection spectra of plasmonic structures.[132–135] Plasmonic spectroscopy can fit into three categories according to the type of plasmonic structures, *i.e.*, surface plasmon resonance (SPR) spectroscopy based on metal thin films, LSPR spectroscopy based on metal nanoparticles, and EOT spectroscopy based on nanohole arrays in metal thin films. We will review these three types of integrated plasmonic spectroscopy devices for enhanced sensing and imaging.

Surface Plasmon Resonance Spectroscopy: Over the past two decades, SPR spectroscopy based on SPPs on metal thin films has attracted attention for its label-free, real-time optical sensing of molecules and affinity interactions between biomolecules. Such spectroscopic sensors are based on the high sensitivity of dispersion of SPPs to the dielectric environments at metal surfaces. SPR sensors have been applied to both SPR spectroscopy and SPR imaging. In order to further miniaturize the sensing system for less reagent consumption and enhanced throughput, tremendous efforts have been made to integrate plasmonic chips into microfluidic systems for parallel multiplexed sensing and imaging.[160–163]

Multiplexed detection is a technology that can minimize detection time by interrogating multiple ligand/analyte interactions in a single device. The parallel and precise sample delivery capability in microfluidics enables the multiplexed detection.[164] For example, Vala *et al.* have demonstrated a compact SPR sensor that is capable of simultaneous detection of up to ten types of analytes based on angular interrogation of SPR on an Au-coated diffraction grating contained in a disposable sensor cartridge with ten independent fluidic channels (Figure 18).[165] The sensor prototype has a detection limit of below 1 nM for short oligonucleotides.

Tremendous progress has also been made in integrating SPR imaging with microfluidic systems. Here, it is worth mentioning that in addition to achieving similar functions as plasmonic spectroscopy, SPR imaging can provide very important spatially-resolved information that plasmonic spectroscopy cannot provide.[166] Lee *et al.* demonstrated the simultaneous detection of multiple hybridization reactions based on SPR imaging integrated with microfluidic systems that include two perpendicular sets of fluidic channels.[167] To

increase the number of independent spots for detection, Luo *et al.* added extra valve systems to selectively open and close certain microfluidic channels to introduce reagents to detection spots independently (Figure 19).[168] With similar valve systems, Ouellet *et al.* have achieved 264 independently addressable microfluidic chambers for SPR imaging, enabling the detection of binding events between multiple analytes and up to 264 different immobilized ligands in a single experiment.[169]

To reduce the complexity of conventional valve systems in microfluidics, other fluidic control technologies such as electrokinetic focusing[170] and electrowetting[171] have been developed for microfluidics-assisted SPR imaging. For example, electrowetting-on-dielectric (EWOD) digital microfluidic technology can manipulate fluids by forming and moving fluid droplets through the electrical modulation of the interfacial tension of droplets, facilitating the SPR imaging-based parallel multiplexed sensing.[172,173] Tabrizian and co-workers have integrated EWOD digital microfluidic technology with SPR imaging for the real-time monitoring of DNA hybridization.[174,175]

Localized Surface Plasmon Resonance Spectroscopy: LSPR spectroscopy uses metal nanoparticles as transducers for optical sensing and imaging applications. Compared with SPR sensors, LSPR spectroscopy has an advantage in the smaller probing volumes that match the size of biomolecules. The integration of LSPR spectroscopy with microfluidics has led to highly miniaturized sensors that enable multiplexed measurements for the high-throughput and high-sensitivity detection of small amounts of analytes, paving the way towards clinical applications.

In the initial demonstration of this “plasmofluidics” concept, Zheng *et al.* developed an LSPR chip integrated with a single microfluidic channel for bulk refractive index sensing.[176] The LSPR properties of plasmonic nanoparticles can be effectively engineered.[177,178] The microfluidic channel alternatively delivers target fluids and rinse fluids to the sensing areas for the quick measurements of optical properties of various fluids. To enhance the sensitivity of LSPR spectroscopy, Sadabadi *et al.* have employed *in-situ* synthesis to generate Au nanoparticles on the sidewalls of microfluidic channels (Figure 20).[179] The LSPR-microfluidic sensor has reached a detection limit of as low as 3.7 ng/ml for bovine growth hormone, providing an alternative approach to protein detection for clinical diagnosis.

To enable automatic transportation of samples and rinse fluids for high-throughput and robust sensing, more sophisticated microfluidic systems with microvalves and micropumps have been integrated with LSPR spectroscopy. Huang *et al.* have developed such sophisticated LSPR-microfluidic spectroscopy to study antigen–antibody reaction and fast hybridization between single-stranded DNA (ssDNA) and complementary target DNA.[180,181] It has been found that the hybridization occurred in 20 minutes under the microfluidic environment, which was much faster than that in a static environment (which takes 3–4 h).[181]

Furthermore, multiplexed immunoassays have been realized by the integration of LSPR substrates with microfluidic systems of multiple channels and microvalves.[182,183] For

example, Quidant and co-workers have developed LSPR sensors that offer 32 parallel sensing sites distributed across 8 independent microfluidic channels (Figure 21).[183] The sensors include microfluidic systems with multiple channels and micromechanical valves bonded onto arrays of Au nanorods immobilized on substrates. The channels ensure precise delivery of analytes among the arrays while the valves allow switching among various modes of operation for the on-chip sensor preparation and sample interrogation. Fast detection of cancer biomarkers at concentrations as low as 500 pg/mL in a complex matrix has been demonstrated with high reproducibility.

Extraordinary Optical Transmission Spectroscopy: EOT is the phenomenon of enhanced transmission of light at certain wavelengths through a subwavelength aperture in an otherwise opaque metal film due to the excitation of SPs.[184,185] Based on the high sensitivity of EOT to changes in the optical properties at the metal-dielectric interfaces, EOT spectroscopy has been utilized for sensing applications. There has been a broad range of research work on EOT sensors based on various plasmonic substrates ranging from long-range ordered nanohole arrays in metal thick films (100 nm)[186] and short-range ordered nanohole arrays in metal thin films (20 nm)[187] to single nanoholes.[188]

Plasmofluidic sensors using EOT substrates integrated with microfluidic platforms have evolved rapidly from single-array, single-channel arrangements to multiplexed arrays of nanoholes and fluidic channels. For example, De Leebeeck *et al.* bonded microfluidic channels onto Au films with nanohole arrays for the spatial-temporal resolved measurements (Figure 22).[189] Both chemical and biological sensing have been demonstrated by monitoring the resonance peak shift in the transmission EOT spectra.

Integration of multiple microfluidic channels into EOT substrates has also allowed the enhanced multiplexed detection based on differential sensing. For example, Oh and co-workers developed and applied high-compact multichannel microarrays that integrate nanohole arrays with six parallel microfluidic channels to realize differential sensing of streptavidin and biotin binding kinetics.[190] Subsequently, the same group integrated twelve microfluidic channels with template-stripped Ag nanohole arrays to achieve a high sensitivity of 3.1×10^{-6} RIU without the use of a temperature-controlled chip or light source.[191–193]

So far, most of EOT sensors have employed the dead-end nanohole arrays in a flow-over format, which cannot harness the benefits of confined transport for chemical or biological sensing. A flow-through format can rapidly transport reactants or analytes to the active surfaces inside the nanoholes, improving the analytical efficiency. Along this line, free-standing nanohole arrays have been developed and integrated with microfluidic platforms for the EOT sensors (Figure 23).[194,195] The flow-through format has exhibited a tremendous improvement in the adsorption kinetics, which is crucial for immunoassay-based applications.[196]

3.2.2 Surface-Enhanced Raman Spectroscopy—Raman spectroscopy is a powerful analytical technique for the “fingerprint” information (vibrational modes) it provides about molecules. When molecules are on or near a roughened metal surface, the Raman signals of

molecules can be enhanced due to the excitation of SPs. This enhancement underpins SERS for high-sensitivity chemical and biochemical analyses.[136–140,197–201] However, the routine use of SERS analysis has remained challenging due to multiple limitations in the conventional SERS devices, including variable mixing times, inhomogeneous distribution of analytes, aggregation of metal nanoparticles, localized heating, and photodissociation of molecules.[202,203] These challenges have been solved by integrating SERS substrates with microfluidic systems that provide precise delivery of analytes, reduce localized heat, and enable a homogeneous mixing of analytes and metal nanoparticles.[204,205]

Docherty *et al.* incorporated the delivery function of microfluidic systems into SERS to achieve the performance-enhanced multiplexed detection of oligonucleotides.[206] As shown in Figure 24, a PDMS microfluidic chip containing three input channels A, B, and C, and one output D is bonded onto a SERS substrate. Channels A and B were used to introduce silver colloid and water, respectively. The pre-mixed analyte and spermine (which was used to aggregate the colloid and neutralize the phosphate backbone in the oligonucleotide) was introduced into channel C. The SERS detection spot is located at position X. This SERS-microfluidic chip has allowed the simultaneous SERS measurements of up to three labeled oligonucleotides. Connatser *et al.* combined a microfluidic separation system with a SERS substrate to realize both separation and detection of targeted analytes.[207] Recently, Fan and coworkers have developed a flow-through microfluidic 3D platform for SERS with the enhanced performances.[208]

Beyond the delivery of fluids and nanoparticles with traditional microfluidic channels with the straight walls, new microfluidic systems have been developed to further improve SERS signals and their reproducibility. For example, Choo and co-workers developed a microfluidic PDMS chip with a teeth-shaped PDMS microfluidic channel to increase the mixing of silver colloids with analytes (Figure 25).[202] Integrating this teeth-shaped microfluidic channel with confocal SERS has enabled the highly sensitive detection of duplex dye-labeled DNA oligonucleotides and cyanide water pollutant.[202–209] Other strategies for enhancing the sensitivity and reliability of microfluidics-based SERS include using capillary forces to trap metal nanoparticles and analytes,[210] creating liquid-core anti-resonant reflecting optical waveguides in a microfluidic chip,[211] and taking advantage of free-surface microfluidic control.[212]

4. Summary and Perspective

The emerging field of plasmofluidics leverages the strengths and advantages of both plasmonics and microfluidics. Whether in the form of plasmon-enhanced functionalities in microfluidic devices or microfluidics-enhanced plasmonic devices, the results presented by many research groups worldwide, thus far, have demonstrated an accelerating pace of progress thanks to rapid advances in micro-/nano-fabrication, chemical synthesis protocols, characterization studies, and numerical simulations. Although plasmofluidics presents great opportunities to observe new physical phenomena and corresponding novel diagnostic applications, current plasmofluidic devices and platforms still require further improvements before they are ready for large-scale implementation of practical applications. We have identified the following opportunities and future directions in the field.

Matching Plasmonics with Nanofluidics

Although the integration of microfluidics with plasmonics has shown tremendous success in enabling new functions and devices, the size mismatch between microfluidic systems and plasmonic nanostructures has become a barrier for further improvements in plasmofluidics. For example, it is challenging for microfluidic systems to manipulate fluids with the same level of controlled precision as with plasmonic nanostructures. The relatively “large” scale in microfluidics has prevented the further miniaturization of current plasmofluidic devices. As a result, the integration of nanofluidics with plasmonics appears to be the next logical step in the development of plasmofluidics. We expect that nanofluidics will enable the confinement of both fluids and light at the nanoscale that will lead to enhanced light-fluid interactions, as well as leading to new physical capabilities and miniaturized devices with novel functionalities. The inevitable integration of nanofluidics with plasmonics is also driven by the great potential for plasmonics to enhance the functionalities of nanofluidics. For example, the plasmon-enhanced heat sources will significantly benefit fluidic manipulations in nanoscale channels due to the remote, nanoscale control of the temperature of fluids.[213–218]

Tuning Metamaterials with Microfluidic Techniques

Metamaterials are artificial optical materials that enable novel manipulations of light.[219–225] Metal nanostructures in a periodic array with a sub-wavelength spacing are one of the most common structures to create metamaterials. By engineering the plasmonic properties of metal nanostructures as building blocks, a broad range of unique capabilities are exhibited that are impossible with conventional optical materials, such as negative refraction,[223,224] ultra-thin metasurfaces,[226–228] and electromagnetic cloaking,[221,229,230] have been implemented. Although there has been tremendous progress in developing various kinds of metamaterials, the lack of dynamic tunability and a narrow spectral response hinder the practical applications of metamaterials. However, the precise control of fluids with variable optical properties within the gap spaces in metamaterials will open up new windows of opportunities for developing tunable, broadband metamaterials. Recent examples include the fluid-enabled enhancement and active tuning of magnetic resonances in free-standing plasmonic metamaterials.[231] We expect a significant boost in this research direction in the near future.

Translating Proof-of-Principle Concepts into Practical Applications

Eventually, the lab demonstration and prototypes of plasmofluidic devices need to be translated into practical applications. It requires innovations in multiple areas in order to move from the proof-of-principle level to real-world practices, including chip fabrication, illumination and detection optics, and system integration. It is highly desired to have simple, single-step, and cost-effective micro-/nano-fabrication techniques that are amenable to mass production of plasmonic and fluidic chips. Such fabrication techniques are emerging. For example, a 3D hierarchical mold fabrication process has been developed to enable monolithic integration of plasmonic gratings within a multichannel microfluidic system.[232] Optical setups for light sources and detection present another critical factor in determining the feasibility of practical plasmofluidic devices. An ideal optical setup should be simple,

compact, robust, and user-friendly. Finally, the system-level design and integration need be developed in order to combine the chips and optical setup into practical plasmofluidic devices that can work reliably in the field environments.

All in all, plasmofluidics is an exciting, highly interdisciplinary field. There are tremendous opportunities for new discoveries and device developments in this field. However, the opportunities are associated with challenges. Due to the interdisciplinary nature of plasmofluidics, to address the upcoming challenges will require tremendous effort from researchers in multiple fields such as optical engineering, electrical engineering, biomedical engineering, mechanical engineering, physics, chemistry, biology, and nanoscience. With the coordinated efforts of various disciplines, advances in the field of plasmofluidics will proliferate rapidly.

Acknowledgments

Y. B. Z. acknowledges financial support from the startup grant from Cockrell School of Engineering at the University of Texas at Austin and the Beckman Young Investigator Program. T. J. H acknowledges financial support from the National Institutes of Health (1R01 GM112048-01A1 and 1R33EB019785-01), the National Science Foundation (CBET-1438126 and IIP-1346440), and the Penn State Center for Nanoscale Science (MRSEC) under grant DMR-0820404. Y. J. L. acknowledges financial support from Agency for Science, Technology and Research (A*STAR), under the grant No. 12302FG012, 0921540098, and 0921540099.

References

1. Raether, H. Surface Plasmons on Smooth and Rough Surfaces and on Gratings. Springer; Berlin, Germany: 1988.
2. Maier, SA. Plasmonics: Fundamentals and Applications. Springer; New York: 2007.
3. Bozhevolnyi, SI. Plasmonic Nanoguides and Circuits. Pan Stanford Publishing Pte. Ltd; Singapore: 2009.
4. Urban AS, Fedoruk M, Horton MR, Rädler JO, Stefani FD, Feldmann J. Nano Lett. 2009; 9:2903. [PubMed: 19719109]
5. Fang C, Shao L, Zhao Y, Wang J, Wu H. Adv Mater. 2012; 24:94. [PubMed: 22144399]
6. Zhang S, Genov DA, Wang Y, Liu M, Zhang X. Phys Rev Lett. 2008; 101:047401. [PubMed: 18764363]
7. Liu N, Langguth L, Weiss T, Kastel J, Fleischhauer M, Pfau T, Giessen H. Nat Mater. 2009; 8:758. [PubMed: 19578334]
8. Gu J, Singh R, Liu X, Zhang X, Ma Y, Zhang S, Maier SA, Tian Z, Azad AK, Chen HT, Taylor AJ, Han J, Zhang W. Nat Commun. 2012; 3:1151. [PubMed: 23093188]
9. Maier SA, Atwater HA. J Appl Phys. 2005; 98:011101.
10. Atwater HA, Polman A. Nat Mater. 2010; 9:205. [PubMed: 20168344]
11. Brolo AG. Nat Photon. 2012; 6:709.
12. Quidant R, Girard C. Laser Photon Rev. 2008; 2:47.
13. http://www.gelifesciences.com/webapp/wcs/stores/servlet/catalog/en/GELifeSciences/brands/biacore/?gclid=Cj0KEQjwyMafBRCU7OCRyc2vitsBEiQAKV4H9BFXB3KbV3Upt_I6lZ3-WF7izuxA0Nwanfxu9p9z_FYaAqmN8P8HAQ
14. http://www.biosensingusa.com/?gclid=Cj0KEQjwyMafBRCU7OCRyc2vitsBEiQAKV4H9OjZ8VGeWnyey9rjFJdWVoxZRqsBhTHWRzaqa4Hbx74aArd48P8HAQ
15. http://www.horiba.com/scientific/products/surface-plasmon-resonance-imaging-spri/
16. Schurig D, Mock JJ, Justice BJ, Cummer SA, Pendry JB, Starr AF, Smith DR. Science. 2006; 314:977. [PubMed: 17053110]
17. Cai W, Chettiar UK, Kildishev AV, Shalaev VM. Nat Photon. 2007; 1:224.

18. Choi Y, Kang T, Lee LP. Nano Lett. 2009; 9:85. [PubMed: 19093833]
19. Lee K, Cui Y, Lee LP, Irudayaraj J. Nat Nanotech. 2014; 9:474.
20. Whitesides GM. Nature. 2006; 442:368. [PubMed: 16871203]
21. Sackmann EK, Fulton AL, Beebe DJ. Nature. 2014; 507:181. [PubMed: 24622198]
22. Abalde-Cela S, Abell C, Alvarez-Puebla RA, Liz-Marzán LM. J Phys Chem Lett. 2014; 5:73. [PubMed: 26276183]
23. Psaltis D, Quake SR, Yang C. Nature. 2006; 442:381. [PubMed: 16871205]
24. Wolfe DB, Conroy RS, Garstecki P, Mayers BT, Fischbach MA, Paul KE, Prentiss M, Whitesides GM. Proc Natl Acad Sci. 2004; 101:12434. [PubMed: 15314232]
25. Domachuk P, Grillet C, Ta'eed V, Mägi E, Bolger J, Eggleton BJ, Rodd LE, Cooper-White J. Appl Phys Lett. 2005; 86:024103.
26. Tang SKY, Stan CA, Whitesides GM. Lab Chip. 2008; 8:395. [PubMed: 18305856]
27. Yang Y, Liu AQ, Chin LK, Zhang XM, Tsai DP, Lin CL, Lu C, Wang GP, Zheludev NI. Nat Commun. 2012; 3:651. [PubMed: 22337129]
28. Mao X, Stratton ZI, Nawaz AA, Lin SCS, Huang TJ. Biomicrofluidics. 2010; 4:043007.
29. Shi J, Stratton Z, Lin SCS, Huang H, Huang TJ. Microfluid Nanofluid. 2010; 9:313.
30. Lapsley MI, Chiang IK, Zheng YB, Ding X, Mao X, Huang TJ. Lab Chip. 2011; 11:1795. [PubMed: 21479332]
31. Zhao Y, Stratton ZS, Guo F, Lapsley MI, Chan CY, Lin SCS, Huang TJ. Lab Chip. 2013; 13:17. [PubMed: 23138193]
32. Mao X, Lin SCS, Dong C, Huang TJ. Lab Chip. 2009; 9:1583. [PubMed: 19458866]
33. Cho SH, Qiao W, Tsai FS, Yamashita K, Lo YH. Appl Phys Lett. 2010; 97:093704. [PubMed: 20877655]
34. Tseng D, Mudanyali O, Oztoprak C, Isikman SO, Sencan I, Yaglidere O, Ozcan A. Lab Chip. 2010; 10:1787. [PubMed: 20445943]
35. Zhu H, Mavandadi S, Coskun AF, Yaglidere O, Ozcan A. Anal Chem. 2011; 83:6641. [PubMed: 21774454]
36. Zhao C, Liu Y, Zhao Y, Fang N, Huang TJ. Nat Commun. 2013; 4:2305. [PubMed: 23929463]
37. Zhao Y, Chen D, Yue H, Spiering M, Zhao C, Benkovic S, Huang TJ. Nano Lett. 2014; 14:1952. [PubMed: 24628474]
38. Li P, Stratton ZS, Dao M, Ritz J, Huang TJ. Lab Chip. 2013; 13:602. [PubMed: 23306378]
39. Zheng YB, Kiraly B, Weiss PS, Huang TJ. Nanomedicine. 2012; 7:751. [PubMed: 22630155]
40. Ashkin A, Dziedzic JM, Bjorkholm JE, Chu S. Opt Lett. 1986; 11:288. [PubMed: 19730608]
41. Grier DG. Nature. 2003; 424:810. [PubMed: 12917694]
42. Moffitt JR, Chemla YR, Smith SB, Bustamante C. Annu Rev Biochem. 2008; 77:205. [PubMed: 18307407]
43. Padgett M, Leonardo RD. Lab Chip. 2011; 11:1196. [PubMed: 21327211]
44. Liu GL, Kim J, Lu Y, Lee LP. Nat Mater. 2006; 5:27. [PubMed: 16362056]
45. Boyd DA, Adleman JR, Goodwin DG, Psaltis D. Anal Chem. 2008; 80:2452. [PubMed: 18321130]
46. Fang C, Shao L, Zhao Y, Wang J, Wu H. Adv Mater. 2012; 24:94. [PubMed: 22144399]
47. Zeng J, Goldfeld D, Xia Y. Angew Chem. 2013; 125:4263.Angew Chem Int Ed. 2013; 52:4169.
48. Miao X, Wilson BK, Lin LY. Appl Phys Lett. 2008; 92:124108.
49. Wagner DS, Delk NA, Lukianova-Hleb EY, Hafner JH, Farach-Carsona MC, Lapotko DO. Biomaterials. 2010; 31:7567. [PubMed: 20630586]
50. Lukianova-Hleb EY, Hanna EY, Hafner JH, Lapotko DO. Nanotechnology. 2010; 21:085102.
51. Kitz M, Preisser S, Wetterwald A, Jaeger M, Thalmann GN, Frenz M. Biomed Opt Express. 2011; 2:291. [PubMed: 21339875]
52. Neumann O, Urban AS, Day J, Lal S, Nordlander P, Halas NJ. ACS Nano. 2013; 7:42. [PubMed: 23157159]

53. Neumann O, Feronti C, Neumann AD, Dong A, Schell K, Lu B, Kim E, Quinne M, Thompso S, Grady N, Nordlander P, Oden M, Halas NJ. Proc Natl Acad Sci. 2013; 110:11677. [PubMed: 23836642]
54. Adleman JR, Boyd DA, Goodwin DG, Psaltis D. Nano Lett. 2009; 9:4417. [PubMed: 19908825]
55. Liu Z, Hung WH, Aykol M, Valley D, Cronin SB. Nanotechnology. 2010; 21:105304. [PubMed: 20160339]
56. Anderson LJE, Hansen E, Lukianova-Hleb EY, Hafner JH, Lapotko DO. J Control Release. 2010; 144:151. [PubMed: 20156498]
57. Li Y, Xu L, Li B. Appl Phys Lett. 2012; 101:053118.
58. Juan ML, Righini M, Quidant R. Nat Photon. 2011; 5:349.
59. Maragò OM, Jones PH, Gucciardi PG, Volpe G, Ferrari AC. Nat Nanotech. 2013; 8:807.
60. Kim J. Lab Chip. 2012; 12:3611. [PubMed: 22858903]
61. Coronado EA, Encinaa ER, Stefani FD. Nanoscale. 2011; 3:4042. [PubMed: 21931921]
62. Donner JS, Baffou G, McCloskey D, Quidant R. ACS Nano. 2011; 5:5457. [PubMed: 21657203]
63. Neuman KC, Chadd EH, Liou GF, Bergman K, Block SM. Biophys J. 1999; 77:2856. [PubMed: 10545383]
64. Volpe G, Quidant R, Badenes G, Petrov D. Phys Rev Lett. 2006; 96:238101. [PubMed: 16803408]
65. Garcés-Chávez V, Quidant R, Reece PJ, Badenes G, Torner L, Dholakia K. Phys Rev B. 2006; 73:085417.
66. Righini M, Zelenina AS, Girard C, Quidant R. Nat Phys. 2007; 3:477.
67. Grigorenko AN, Roberts NW, Dickinson MR, Zhang Y. Nat Photon. 2008; 2:365.
68. Righini M, Ghenuche P, Cherukulappurath S, Myroshnychenko V, García de Abajo FJ, Quidant R. Nano Lett. 2009; 9:3387. [PubMed: 19159322]
69. Rasmussen MB, Oddershede LB, Siegumfeldt H. Appl Environ Microbio. 2008; 74:2441.
70. Zhang W, Huang L, Santschi C, Martin OJF. Nano Lett. 2010; 10:1006. [PubMed: 20151698]
71. Tsuboi Y, Shoji T, Kitamura N, Takase M, Murakoshi K, Mizumoto Y, Ishihara H. J Phys Chem Lett. 2010; 1:2327.
72. Ureña EB, Kreuzer MP, Itzhakor S, Rigneault H, Quidant R, Oron D, Wenger J. Adv Mater. 2012; 24:OP314. [PubMed: 23027548]
73. Galloway CM, Kreuzer MP, Aćimović SS, Volpe G, Correia M, Petersen SB, Neves-Petersen MT, Quidant R. Nano Lett. 2013; 13:4299. [PubMed: 23915079]
74. Saleh AAE, Dionne JA. Nano Lett. 2012; 12:5581. [PubMed: 23035765]
75. Juan ML, Gordon R, Pang Y, Eftekhari F, Quidant R. Nat Phys. 2009; 5:915.
76. Chen C, Juan ML, Li Y, Maes G, Borghs G, Dorpe PV, Quidant R. Nano Lett. 2012; 12:125. [PubMed: 22136462]
77. Pang Y, Gordon R. Nano Lett. 2011; 11:3763. [PubMed: 21838243]
78. Pang Y, Gordon R. Nano Lett. 2012; 12:402. [PubMed: 22171921]
79. Zehtabi-Oskuie A, Jiang H, Cyr BR, Rennehan DW, AlBalushi AA, Gordon R. Lab Chip. 2013; 13:2563. [PubMed: 23429640]
80. Zehtabi-Oskuie A, Bergeron JG, Gordon R. Sci Rep. 2012; 2:966. [PubMed: 23236587]
81. Kotnala A, Gordon R. Nano Lett. 2014; 14:853. [PubMed: 24404888]
82. Berthelot J, Aćimović SS, Juan ML, Kreuzer MP, Renger J, Quidant R. Nat Nanotech. 2014; 9:295.
83. Roxworthy BJ, Ko KD, Kumar A, Fung KH, Chow EKC, Liu GL, Fang NX, Toussaint KC Jr. Nano Lett. 2011; 12:796. [PubMed: 22208881]
84. Shoji T, Shibata M, Kitamura N, Nagasawa F, Takase M, Murakoshi K, Nobuhiro A, Mizumoto Y, Ishihara H, Tsuboi Y. J Phys Chem C. 2013; 117:2500.
85. Roxworthy BJ, Bhuiya AM, Vanka SP, Toussaint KC Jr. Nat Commun. 2014; 5:3173. [PubMed: 24445431]
86. Wang K, Schonbrun E, Steinvurzel P, Crozier KB. Nat Commun. 2011; 2:469. [PubMed: 21915111]

87. Kang JH, Kim K, Ee HS, Lee YH, Yoon TY, Seo MK, Park HG. Nat Commun. 2011; 2:582. [PubMed: 22158437]
88. Roxworthy BJ, Toussaint KC Jr. Sci Rep. 2012; 2:660. [PubMed: 22993686]
89. Shoji T, Saitoh J, Kitamura N, Nagasawa F, Murakoshi K, Yamauchi H, Ito S, Miyasaka H, Ishihara H, Tsuboi Y. J Am Chem Soc. 2013; 135:6643. [PubMed: 23586869]
90. Lovera A, Martin OJF. Appl Phys Lett. 2011; 99:151104.
91. Kotnala A, DePaoli D, Gordon R. Lab Chip. 2013; 13:4142. [PubMed: 23969596]
92. Wang K, Schonbrun E, Steinvurzel P, Crozier KB. Nano Lett. 2010; 10:3506. [PubMed: 20715811]
93. Ploschner M, Čizma T, Mazilu M, Di Falco A, Dholakia K. Nano Lett. 2012; 12:1923. [PubMed: 22448854]
94. Min C, Shen Z, Shen J, Zhang Y, Fang H, Yuan G, Du L, Zhu S, Lei T, Yuan X. Nat Commun. 2013; 4:2891. [PubMed: 24305554]
95. Bozhevolnyi SI, Volkov VS, Devaux E, Laluet JY, Ebbesen TW. Nature. 2006; 440:508. [PubMed: 16554814]
96. Zentgraf T, Liu Y, Mikkelsen MH, Valentine J, Zhang X. Nat Nanotech. 2011; 6:151.
97. Zhao C, Zhang J. ACS Nano. 2010; 4:6433. [PubMed: 20925325]
98. Verslegers L, Catrysse PB, Yu Z, White JS, Barnard ES, Brongersma ML, Fan S. Nano Lett. 2009; 9:235. [PubMed: 19053795]
99. Gao H, Hyun JK, Lee MH, Yang JC, Lauhon LJ, Odom TW. Nano Lett. 2010; 10:4111. [PubMed: 20839781]
100. Ishii S, Shalaev VM, Kildishev AV. Nano Lett. 2013; 13:159. [PubMed: 23244006]
101. Liu YJ, Liu H, Leong ESP, Chum CC, Teng JH. Adv Opt Mater. 2014; 2:487.
102. Lezec HJ, Dionne JA, Atwater HA. Science. 2007; 316:430. [PubMed: 17379773]
103. Xiao S, Drachev VP, Kildishev AV, Ni X, Chettiar UK, Yuan HK, Shalaev VM. Nature. 2010; 466:735. [PubMed: 20686570]
104. Pendry JB. Phys Rev Lett. 2000; 85:3966. [PubMed: 11041972]
105. Fang N, Lee H, Sun C, Zhang X. Science. 2005; 308:534. [PubMed: 15845849]
106. Kehr SC, Liu YM, Martin LW, Yu P, Gajek M, Yang SY, Yang CH, Wenzel MT, Jacob R, von Ribbeck HG, Helm M, Zhang X, Eng LM, Ramesh R. Nat Commun. 2011; 2:249. [PubMed: 21427720]
107. Lu D, Liu Z. Nat Commun. 2012; 3:1205. [PubMed: 23149749]
108. Wang J, Liu S, Nahata A. Opt Express. 2012; 20:12119. [PubMed: 22714198]
109. Fang Z, Zhen Y-R, Neumann O, Polman A, García de Abajo FJ, Nordlander P, Halas NJ. Nano Lett. 2013; 13:1736. [PubMed: 23517407]
110. Lukianova-Hleb E, Hu Y, Latterini L, Tarpani L, Lee S, Drezek RA, Hafner JH, Lapotko DO. ACS Nano. 2010; 4:2109. [PubMed: 20307085]
111. Lapotko DO. Opt Express. 2009; 17:2538. [PubMed: 19219157]
112. Kossyrev PA, Yin A, Cloutier SG, Cardimona DA, Huang D, Alsing PM, Xu JM. Nano Lett. 2005; 5:1978. [PubMed: 16218721]
113. Hsiao VKS, Zheng YB, Juluri BK, Huang TJ. Adv Mater. 2008; 20:3528.
114. Liu YJ, Hao Q, Smalley JST, Liou J, Khoo IC, Huang TJ. Appl Phy Lett. 2010; 97:091101.
115. Liu YJ, Leong ESP, Wang B, Teng JH. Plasmonics. 2011; 6:659.
116. Liu YJ, Zheng YB, Liou J, Chiang IK, Khoo IC, Huang TJ. J Phys Chem C. 2011; 115:7717.
117. Hao Q, Zhao Y, Juluri BK, Kiraly B, Liou J, Khoo IC, Huang TJ. J Appl Phys. 2011; 109:084340.
118. Khatua S, Chang WS, Swanglap P, Olson J, Link S. Nano Lett. 2011; 11:3797. [PubMed: 21861468]
119. Liu YJ, Si GY, Leong ESP, Xiang N, Danner AJ, Teng JH. Adv Mater. 2012; 24:OP131. [PubMed: 22438069]
120. Liu Q, Cui Y, Gardner D, Li X, He S, Smalyukh II. Nano Lett. 2010; 10:1347. [PubMed: 20334353]
121. Kasirga TS, Ertas YN, Bayindir M. Appl Phys Lett. 2009; 95:214102.

122. Vivekchand SRC, Engel CJ, Lubin SM, Blaber MG, Zhou W, Suh JY, Schatz GC, Odom TW. Nano Lett. 2012; 12:4324. [PubMed: 22823536]
123. Cecchini MP, Turek VA, Paget J, Kornyshev AA, Edel JB. Nat Mater. 2013; 12:165. [PubMed: 23160268]
124. Edel JB, Kornyshev AA, Urbakh M. ACS Nano. 2013; 7:9526. [PubMed: 24237248]
125. Turek VA, Elliott LN, Tyler AII, Demetriadou A, Paget J, Cecchini MP, Kucernak AR, Kornyshev AA, Edel JB. ACS Nano. 2013; 7:8753. [PubMed: 24070428]
126. Fang PP, Chen S, Deng H, Scanlon MD, Gumy F, Lee HJ, Momotenko D, Amstutz V, Cortés-Salazar F, Pereira CM, Yang Z, Girault HH. ACS Nano. 2013; 7:9241. [PubMed: 24047434]
127. Perron D, Wu M, Horvath C, Bachman D, Van V. Opt Lett. 2011; 36:2731. [PubMed: 21765524]
128. Dicken MJ, Sweatlock LA, Pacifici D, Lezec HJ, Bhattacharya K, Atwater HA. Nano Lett. 2008; 8:4048. [PubMed: 18847247]
129. Dionne JA, Diest K, Sweatlock LA, Atwater HA. Nano Lett. 2009; 9:897. [PubMed: 19170558]
130. MacDonald KF, Sámson ZL, Stockman MI, Zheludev NI. Nat Photon. 2009; 3:55.
131. Suh JY, Donev EU, Lopez R, Feldman LC, Haglund RF. Appl Phys Lett. 2006; 88:133115.
132. Nylander C, Liedberg B, Lind T. Sens Actuators. 1982–1983; 3:79.
133. Liedberg B, Nylander C, Lundstrom I. Sens Actuators. 1983; 4:299.
134. Homola J, Yee SS, Gauglitz G. Sens Actuators B Chem. 1999; 54:3.
135. Homola J. Chem Rev. 2008; 108:462. [PubMed: 18229953]
136. Wei Y, Cao C, Jin R, Mirkin CA. Science. 2002; 297:1536. [PubMed: 12202825]
137. Ding Y, Fan FR, Huang YF, Li JF, Li SB, Ren B. Nature. 2010; 464:392. [PubMed: 20237566]
138. Oh Y-J, Jeong K-H. Lab Chip. 2014; 14:865. [PubMed: 24452813]
139. Parisi J, Su L, Lei Yu. Lab Chip. 2013; 13:1501. [PubMed: 23459704]
140. Wang Y, Yan B, Chen L. Chem Rev. 2013; 113:1391. [PubMed: 23273312]
141. Wang J, Liu S, Vardeny ZV, Nahata A. Opt Express. 2012; 20:2346. [PubMed: 22330473]
142. Si GY, Zhao YH, Leong ESP, Liu YJ. Materials. 2014; 7:1296.
143. Liu YJ, Sun XW. Appl Phys Lett. 2007; 90:191118.
144. Liu YJ, Dai HT, Leong ESP, Teng JH, Sun XW. Appl Phys B. 2011; 104:659.
145. Liu YJ, Zheng YB, Shi J, Huang H, Walker TR, Huang TJ. Opt Lett. 2009; 34:2351. [PubMed: 19649094]
146. Liu YJ, Cai ZY, Leong ESP, Zhao XS, Teng JH. J Mater Chem. 2012; 22:7609.
147. Liu YJ, Su YC, Hsu YJ, Hsiao VKS. J Mater Chem. 2012; 22:14191.
148. Liu YJ, Ding XY, Lin SCS, Shi JJ, Chiang IK, Huang TJ. Adv Mater. 2011; 23:1656. [PubMed: 21438028]
149. Chang WS, Lassiter JB, Swanglap P, Sobhani H, Khatua S, Nordlander P, Halas NJ, Link S. Nano Lett. 2012; 12:4977. [PubMed: 22924610]
150. Hor YL, Szabó Z, Lim HC, Federici JF, Li EP. Appl Opt. 2010; 49:1179. [PubMed: 20220872]
151. Krasavin AV, Zheludev NI. Appl Phys Lett. 2004; 84:1416.
152. Haes AJ, Van Duyne RP. J Am Chem Soc. 2002; 124:10596. [PubMed: 12197762]
153. Nath N, Chilkoti A. Anal Chem. 2002; 74:504. [PubMed: 11838667]
154. Zhang N, Liu YJ, Yang J, Su XD, Deng J, Chum CC, Hong MH, Teng JH. Nanoscale. 2014; 6:1416. [PubMed: 24311121]
155. Mello LD, Kubota LT. Food Chem. 2002; 77:237.
156. Leonard P, Hearty S, Brennan J, Dunne L, Quinn J, Chakraborty T, O'Kennedy R. Enzyme Microb Tech. 2003; 32:3.
157. Waswa J, Irudayaraj J, DebRoy C. LWT-Food Sci Technol. 2007; 40:187.
158. Rogers KR. Anal Chim Acta. 2006; 568:222. [PubMed: 17761264]
159. Wang L, Zhu Y, Xu L, Chen W, Kuang H, Liu L, Agarwal A, Xu C, Kotov NA. Angew Chem. 2010; 122:5604.Angew Chem Int Ed. 2010; 49:5472.
160. Furuki M, Kameoka J, Craighead HG, Isaacson MS. Sens Actuators B Chem. 2001; 79:63.

161. Lee HJ, Goodrich TT, Corn RM. Anal Chem. 2001; 73:5525. [PubMed: 11816583]
162. Wheeler AR, Chah S, Whelan RJ, Zare RN. Sens Actuators B Chem. 2004; 98:208.
163. Kanda V, Kariuki JK, Harrison DJ, McDermott MT. Anal Chem. 2004; 76:7257. [PubMed: 15595867]
164. Springer T, Piliarik M, Homola J. Sens Actuators B Chem. 2010; 145:588.
165. Vala M, Chadt K, Piliarik M, Homola J. Sens Actuators B Chem. 2010; 148:544.
166. Campbell CT, Kim G. Biomater. 2007; 28:2380.
167. Lee HJ, Goodrich TT, Corn RM. Anal Chem. 2001; 73:5525. [PubMed: 11816583]
168. Luo Y, Yu F, Zare RN. Lab Chip. 2008; 8:694. [PubMed: 18432338]
169. Ouellet E, Lausted C, Lin T, Yang CW, Hood L, Lagally ET. Lab Chip. 2010; 10:581. [PubMed: 20162233]
170. Krishnamoorthy G, Carlen ET, de Boer HL, van den Berg A, Schasfoort RB. Anal Chem. 2010; 82:4145. [PubMed: 20402468]
171. Lee J, Moon H, Fowler J, Schoellhammer T, Kim CJ. Sens Actuators A Phys. 2002; 95:259.
172. Fair RB. Microfluid Nanofluidics. 2007; 3:245.
173. Cho SK, Moon H, Kim CJ. J Microelectromech Syst. 2003; 12:70.
174. Malica L, Veres T, Tabrizian M. Biosens Bioelectron. 2009; 24:2218. [PubMed: 19136248]
175. Malic L, Veres T, Tabrizian M. Lab Chip. 2009; 9:473. [PubMed: 19156299]
176. Zheng YB, Juluri BK, Mao X, Walker TR, Huang TJ. J Appl Phys. 2008; 103:014308.
177. Zheng YB, Huang TJ, Desai AY, Wang SJ, Tan LK, Gao H, Huang ACH. Appl Phys Lett. 2007; 90:183117.
178. Juluri BK, Zheng YB, Ahmed D, Jensen L, Huang TJ. J Phys Chem C. 2008; 112:7309.
179. SadAbadi H, Badilescu S, Packirisamy M, Wuthrich R. Biosens Bioelectron. 2013; 44:77. [PubMed: 23395726]
180. Huang C, Bonroy K, Reekman G, Verstreken K, Lagae L, Borghs G. Microelectron Eng. 2009; 86:2437.
181. Huang C, Ye J, Wang S, Stakenborg T, Lagae L. Appl Phys Lett. 2012; 100:173114.
182. Zhang Y, Tang Y, Hsieh YH, Hsu CY, Xi J, Lin KJ, Jiang X. Lab Chip. 2012; 12:3012. [PubMed: 22772076]
183. Aćimović SS, Ortega MA, Sanz V, Berthelot J, Garcia-Cordero JL, Renger J, Maerkl SJ, Kreuzer MP, Quidan R. Nano Lett. 2014; 14:2636. [PubMed: 24730454]
184. Ebbesen TW, Lezec HJ, Ghaemi HF, Thio T, Wolff PA. Nature. 1998; 391:667.
185. Genet C, Ebbesen TW. Nature. 2007; 445:39. [PubMed: 17203054]
186. Brolo AG, Gordon R, Leathem B, Kavanagh KL. Langmuir. 2004; 20:4813. [PubMed: 15984236]
187. Dahlin AB, Zach M, Rindzevicius T, Kall M, Sutherland DS, Hook F. J Am Chem Soc. 2005; 127:5043. [PubMed: 15810838]
188. Rindzevicius T, Alaverdyan Y, Dahlin AB, Hook F, Sutherland DS, Kall M. Nano Lett. 2005; 5:2335. [PubMed: 16277479]
189. De Leebeeck A, Kumar LKS, de Lange V, Sinton D, Gordon R, Brolo AG. Anal Chem. 2007; 79:4094. [PubMed: 17447728]
190. Im H, Lesuffleur A, Lindquist NC, Oh SH. Anal Chem. 2009; 81:2854. [PubMed: 19284776]
191. Im H, Lee SH, Wittenberg NJ, Johnson TW, Lindquist NC, Nagpal P, Norris DJ, Oh SH. ACS Nano. 2011; 5:6244. [PubMed: 21770414]
192. Nagpal P, Lindquist NC, Oh SH, Norris DJ. Science. 2009; 325:594. [PubMed: 19644116]
193. Im H, Sutherland JN, Maynard JA, Oh SH. Anal Chem. 2012; 84:1941. [PubMed: 22235895]
194. Eftekhari F, Escobedo C, Ferreira J, Duan X, Girotto EM, Brolo AG, Gordon R, Sinton D. Anal Chem. 2009; 81:4308. [PubMed: 19408948]
195. Yanik AA, Huang M, Artar A, Chang TY, Altug H. Appl Phys Lett. 2010; 96:021101.
196. Squires TM, Messinger RJ, Manalis SR. Nat Biotechnol. 2008; 26:417. [PubMed: 18392027]
197. Pathem BK, Zheng YB, Morton S, Petersen MA, Zhao Y, Chung CH, Yang Y, Jensen L, Nielsen MB, Weiss PS. Nano Lett. 2013; 13:337. [PubMed: 23286277]

198. Zheng YB, Payton JL, Song TB, Pathem BK, Zhao Y, Ma H, Yang Y, Jensen L, Jen AKY, Weiss PS. Nano Lett. 2012; 12:5362. [PubMed: 22978482]
199. Pathem BK, Zheng YB, Payton JL, Song TB, Yu BC, Tour JM, Yang Y, Jensen L, Weiss PW. J Phys Chem Lett. 2012; 3:2388. [PubMed: 26292120]
200. Zheng YB, Kiraly B, Weiss PW, Huang TJ. Nanomedicine. 2012; 7:751. [PubMed: 22630155]
201. Zheng YB, Payton JL, Chung CH, Liu R, Cheunkar S, Pathem BK, Yang Y, Jensen L, Weiss PS. Nano Lett. 2011; 11:3447. [PubMed: 21749070]
202. Park T, Lee S, Seong GH, Choo J, Lee EK, Kim YS, Ji WH, Hwang SY, Gweon DG, Lee S. Lab Chip. 2005; 5:437. [PubMed: 15791342]
203. Lee S, Choi J, Chen L, Park B, Kyong JB, Seong GH, Choo J, Lee Y, Shin KH, Lee EK, Joo SW, Lee KH. Analytica Chimica Acta. 2007; 590:139. [PubMed: 17448337]
204. Fan X, White IM. Nat Photon. 2011; 5:591.
205. White IM, Yazdi SH, Yu WW. Microfluid Nanofluid. 2012; 12:205.
206. Docherty FT, Monaghan PB, Keir R, Graham D, Smith WE, Cooper JM. Chem Commun. 2004:118.
207. Connatser RM, Riddle LA, Sepaniak MJ. J Sep Sci. 2004; 27:1545. [PubMed: 15638165]
208. Guo Y, Oo MKK, Reddy K, Fan X. ACS Nano. 2012; 6:381. [PubMed: 22176766]
209. Yea KH, Lee S, Kyong JB, Choo J, Lee EK, Joo SW, Lee S. Analyst. 2005; 130:1009. [PubMed: 15965522]
210. Wang M, Jing N, Chou IH, Cote GL, Kameoka J. Lab Chip. 2007; 7:630. [PubMed: 17476383]
211. Measor P, Seballos L, Yin D, Zhang JZ, Lunt EJ, Hawkins AR, Schmidt H. Appl Phys Lett. 2007; 90:211107.
212. Piorek BD, Lee SJ, Santiago JG, Moskovits M, Banerjee S, Meinhart CD. Proc Natl Acad Sci. 2007; 104:18898. [PubMed: 18025462]
213. Baffou G, Girard C, Quidant R. Phys Rev Lett. 2010; 104:136805. [PubMed: 20481904]
214. Baffou G, Quidant R, García de Abajo FJ. ACS Nano. 2010; 4:709. [PubMed: 20055439]
215. Herzog JB, Knight MW, Natelson D. Nano Lett. 2014; 14:499. [PubMed: 24382140]
216. Baffou G, Berto P, Bermúdez Ureña E, Quidant R, Monneret S, Polleux J, Rigneault H. ACS Nano. 2013; 7:6478. [PubMed: 23895209]
217. Sanchot A, Baffou G, Marty R, Arbouet A, Quidant R, Girard C, Dujardin E. ACS Nano. 2012; 6:3434. [PubMed: 22394263]
218. Baffou G, Quidant R. Laser Photon Rev. 2013; 7:171.
219. Engheta N. Science. 2007; 317:1698. [PubMed: 17885123]
220. Shalaev VM. Nat Photon. 2007; 1:41.
221. Liu R, Ji C, Mock JJ, Chin JY, Cui TJ, Smith DR. Science. 2009; 323:366. [PubMed: 19150842]
222. Driscoll T, Kim H-T, Chae B-G, Kim B-J, Lee Y-W, Marie Jokerst N, Palit S, Smith DR, Di Ventra M, Basov DN. Science. 2009; 325:1518. [PubMed: 19696311]
223. Valentine J, Zhang S, Zentgraf T, Ulin-Avila E, Genov DA, Bartal G, Zhang X. Nature. 2008; 455:376. [PubMed: 18690249]
224. Xiao S, Drachev VP, Kildishev AV, Ni X, Chettiar UK, Yuan HK, Shalaev VM. Nature. 2010; 466:735. [PubMed: 20686570]
225. Lu D, Kan JJ, Fullerton EE, Liu Z. Nat Nanotech. 2014; 9:48.
226. Yu N, Genevet P, Kats MA, Aieta F, Tetienne JP, Capasso F, Gaburro Z. Science. 2011; 334:333. [PubMed: 21885733]
227. Aieta F, Genevet P, Kats MA, Yu N, Blanchard R, Gaburro Z, Capasso F. Nano Lett. 2012; 12:4932. [PubMed: 22894542]
228. Kildishev AV, Boltasseva A, Shalaev VM. Science. 2013; 339:1232009. [PubMed: 23493714]
229. Chen X, Luo Y, Zhang J, Jiang K, Pendry JB, Zhang S. Nat Commun. 2011; 2:176. [PubMed: 21285954]
230. Landy N, Smith DR. Nat Mater. 2013; 12:25. [PubMed: 23142840]

231. Leong ESP, Liu YJ, Deng J, Fong YT, Zhang N, Wu SJ, Teng JH. Nanoscale. 2014; 6:11106. [PubMed: 25213571]

232. Malic L, Morton K, Clime L, Veres T. Lab Chip. 2013; 13:798. [PubMed: 23287840]

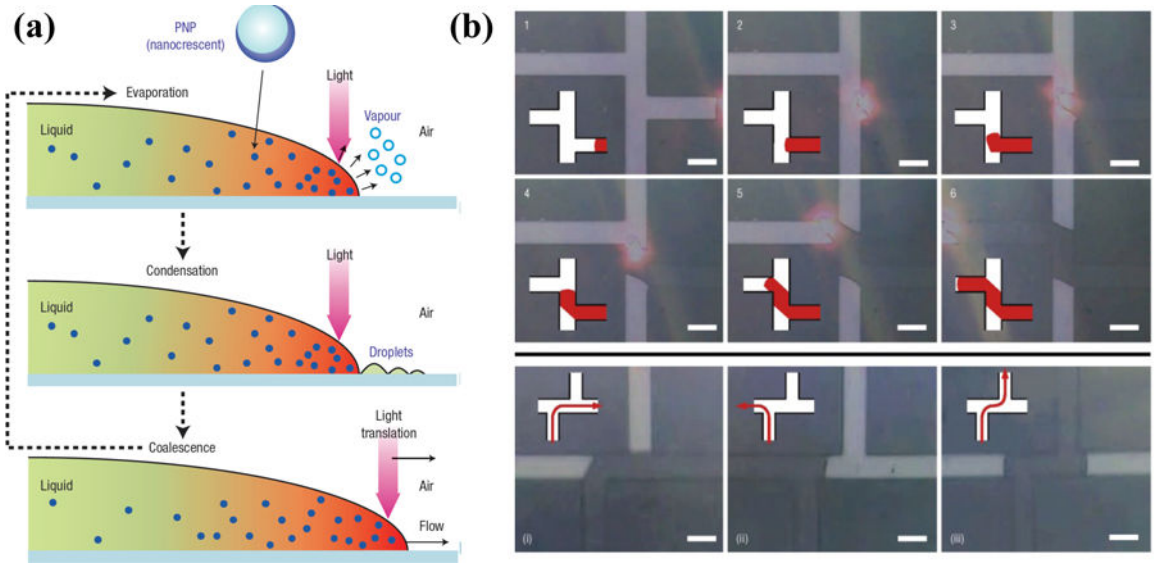

Figure 1.

(a) Schematic illustration of the working principle of the optically controlled fluid flow based on the plasmon-enhanced photothermal effects of metal nanoparticles. (b) Successive optical images show that the fluid flow can be optically guided into desired channels. Reprinted with permission from ref. 44. Copyright (2006) Nature Publishing Group.

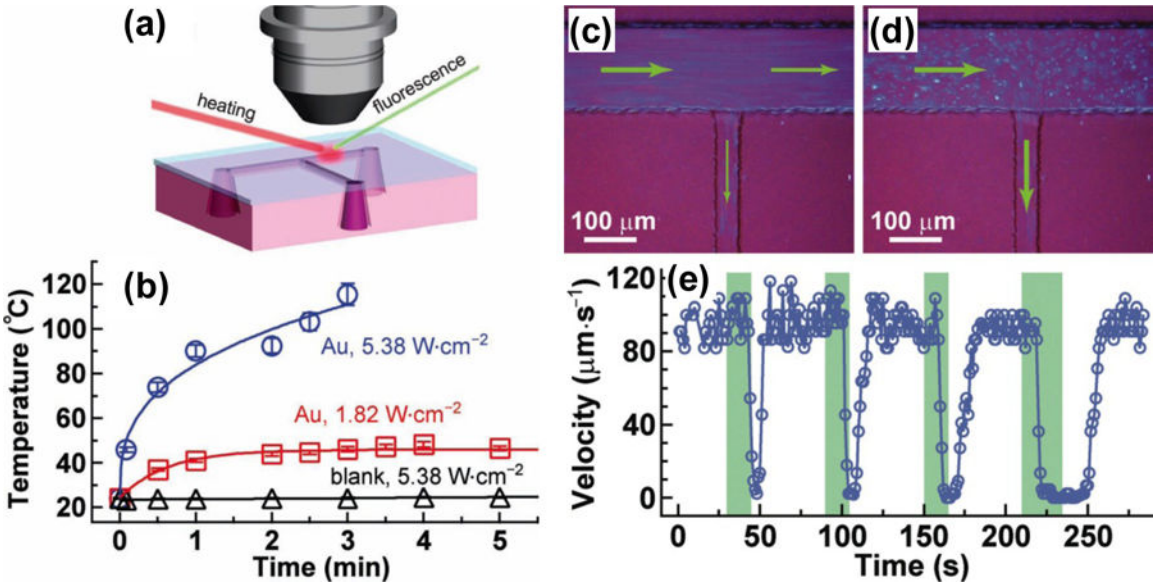

Figure 2.

(a) Schematic of the experimental setup for the evaluation of photothermal heating in PDMS channels embedded with Au nanoparticles. (b) Temperature increase curves of fluids containing either the Au nanorod/PDMS composite or pure PDMS. (c) Image shows that both the outlet channels are on. (d) Image shows that the right outlet channel is off while the side outlet channel is on. The green arrows indicate the flow directions. (e) Plot of the fluid flow velocity inside the right outlet channel versus time. The green bars represent the time periods of the laser illumination on the right outlet channel. Reprinted with permission from ref. 46. Copyright (2012) Wiley-VCH.

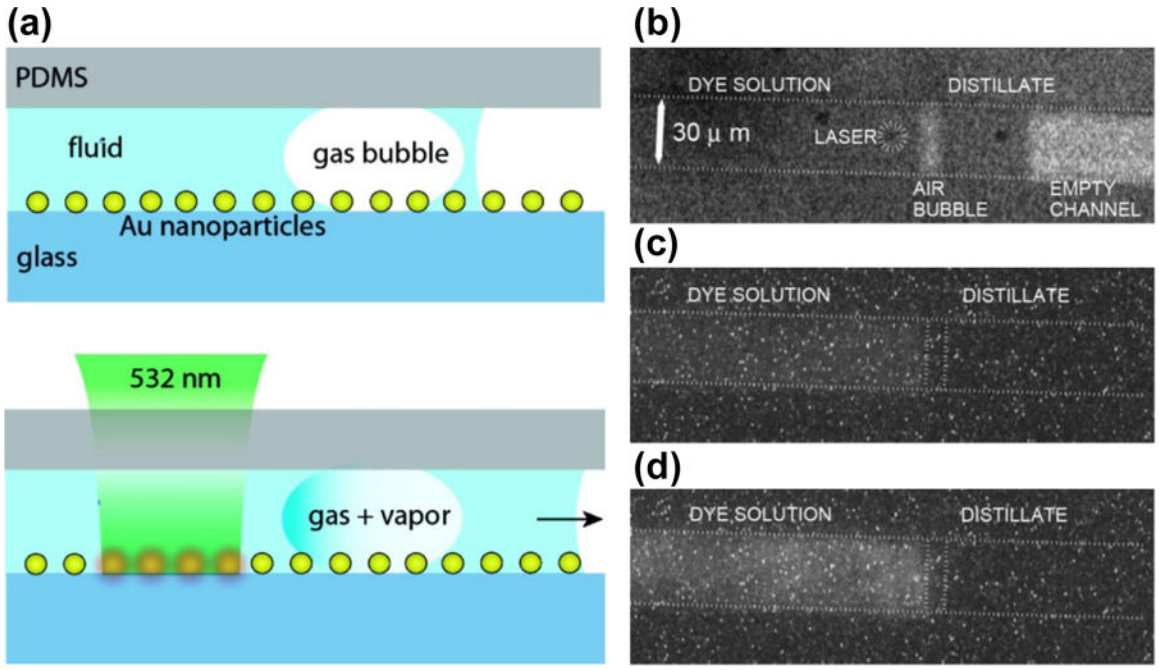

Figure 3.

(a) Schematic illustration of the separation and distillation of microscale liquids based on LSPR-induced photothermal effects combined with the bubble-assisted interphase mass-transfer. (b–d) The optical images reveal the processes involved in the BAIM distillation. Reprinted with permission from ref. 45. Copyright (2008) American Chemical Society.

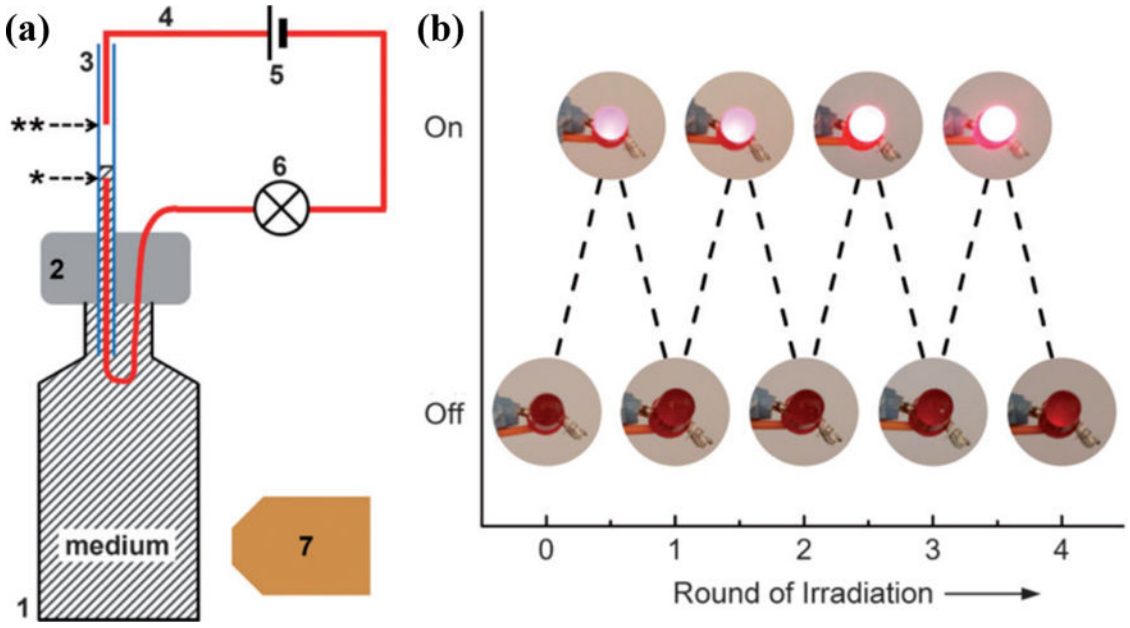

Figure 4.

(a) Schematic illustration of an electrical switch based on photothermal control of fluid flow in the capillary tube (**3**). The capillary tube was inserted into a PDMS block (**2**) capped on a 5 mL glass vial. The batteries (**5**) were connected in series to a standard LED light bulb (**6**) with standard copper wires (**4 in red**). There was a gap between the two copper wires. When the vial was irradiated with a laser beam (**7**), the solution expanded, filled the capillary tube, and bridged the gap between the two copper wires, turning on the LED bulb. (b) Experimental demonstration of the on–off reversible photoswitching of an LED. Reprinted with permission from ref. 47. Copyright (2013) Wiley-VCH.

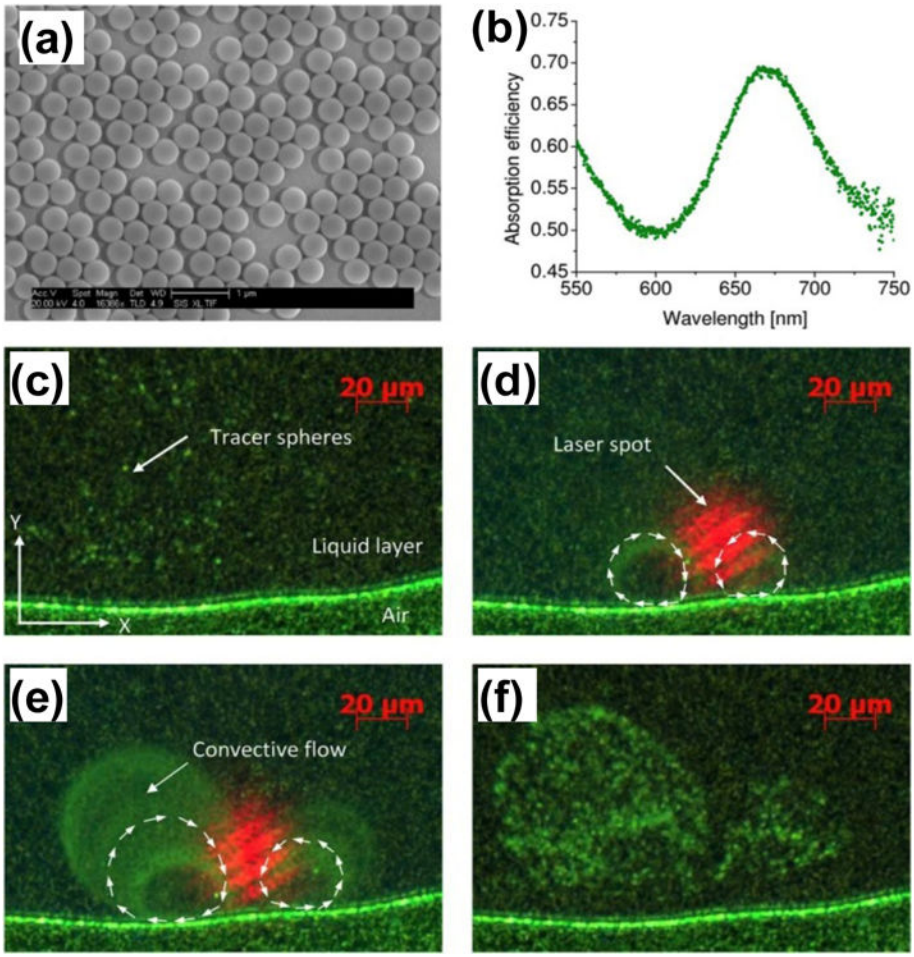

Figure 5.

(a) SEM micrograph of the cap-shaped Au nanoparticle array substrate used for the photothermal mixing. (b) Absorption spectrum of the cap-shaped Au nanoparticle array with the peak located at ~670 nm. (c–f) Optical images reveal the plasmon-enhanced optical mixing. Reprinted with permission from ref. 48. Copyright (2008) American Institute of Physics.

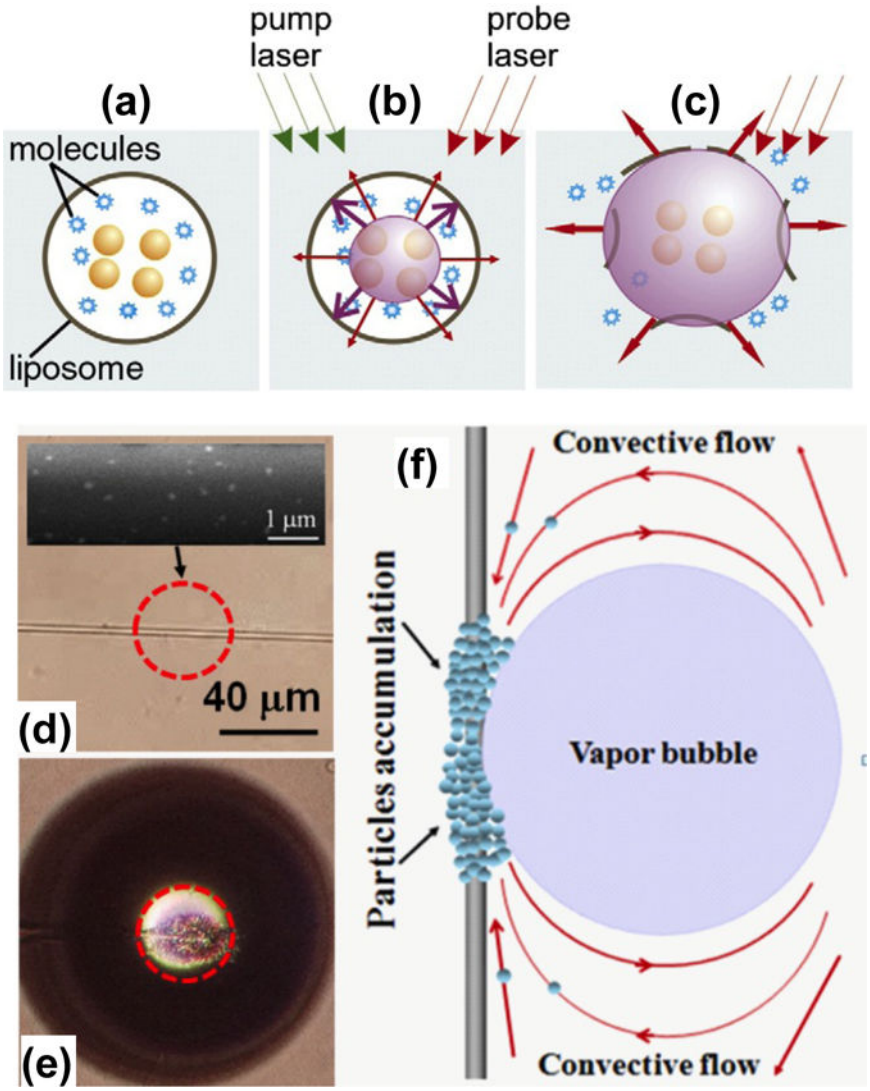

Figure 6.

Schematic illustration of bubble generation and applications based on plasmon-enhanced photothermal effects. (a–c) Optically guided controlled-release of encapsulated molecules. Reprinted with permission from ref. 56. Copyright (2010) Elsevier. (d–f) Microparticle aggregation on the targeted site of the tapered optical fiber due to the plasmon-assisted bubble generation and Marangoni convection. Reprinted with permission from ref. 57. Copyright (2012) American Institute of Physics.

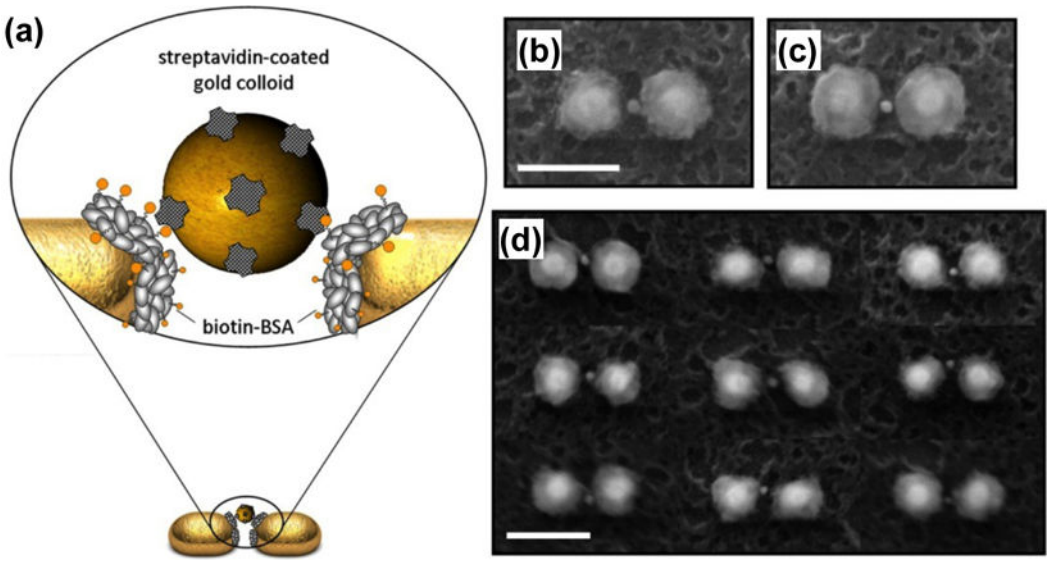

Figure 7.

(a) Schematic of a single Au nanocolloid binding to an immobilized protein in the gap of a Au dimer. (b) and (c) Scanning electron microscopy (SEM) images show binding of a single Au nanocolloid in the gap of Au dimers. (d) SEM image illustrates the self-alignment of Au colloids in hot spots, despite morphological irregularities of the hosting dimers (scale bar: 150 nm). Reprinted with permission from ref. 73. Copyright (2013) American Chemical Society.

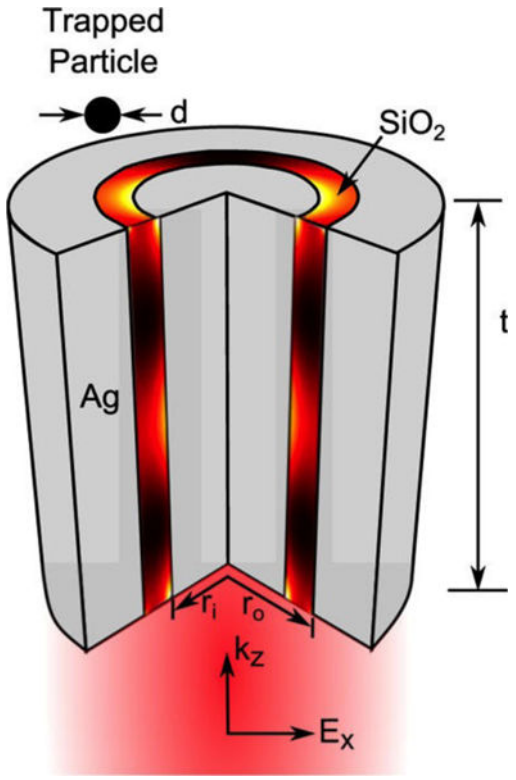

Figure 8.
Schematic of the coaxial plasmonic aperture (a dielectric ring embedded in a noble metal). Reprinted with permission from ref. 74. Copyright (2012) American Chemical Society.

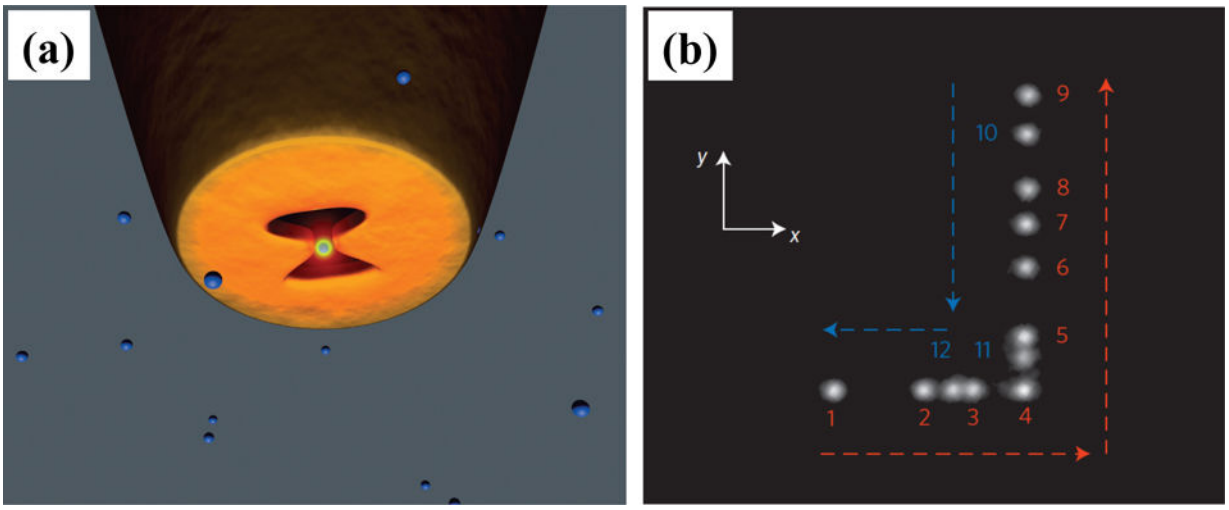

Figure 9.

(a) Schematic of a bowtie nano-aperture at the tip of a metal-coated tapered optical fiber probe used for SIBA optical 3D manipulation. The trapping laser is directly coupled into the fiber to excite the transverse mode of the aperture. (b) A composite image reveals the displacement of the trapped object. Numbers 1–12 represent the successive steps of the tip movement during the time period t = 180–210 s. Reprinted with permission from ref. 82. Copyright (2014) Nature Publishing Group.

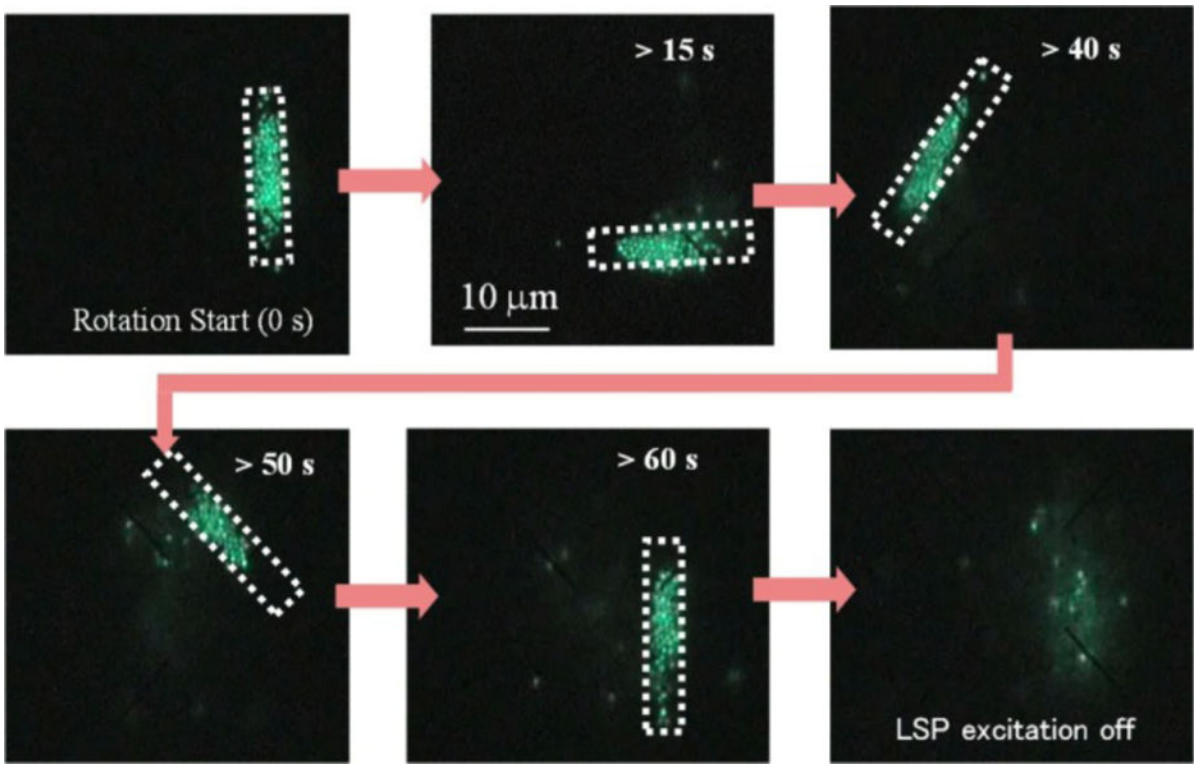

Figure 10.

Successive fluorescent images reveal the manipulation of polystyrene nanospheres based on arrays of Au nanopyramidal dimers. Changing the profile of irradiation light enabled the dynamic manipulation. Reprinted with permission from ref. 84. Copyright (2013) American Chemical Society.

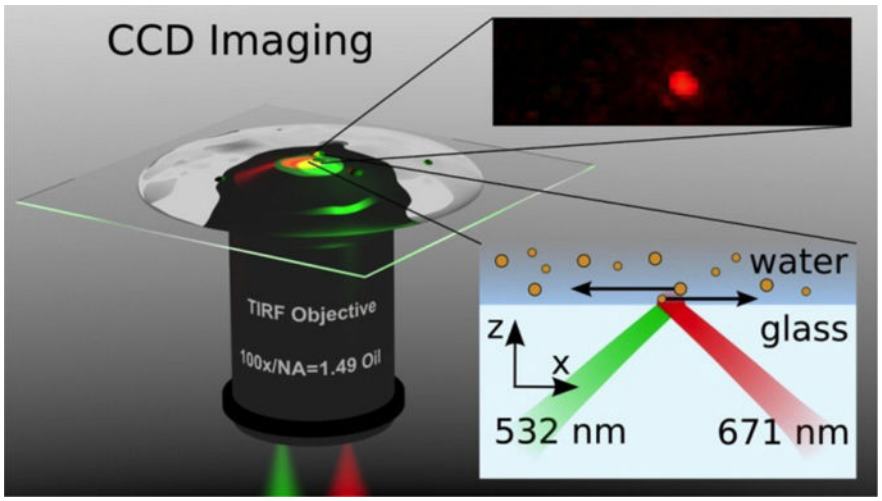

Figure 11.

Schematic of sorting Au nanoparticles with two counter-propagating evanescent waves excited with laser beams of different wavelengths (532 nm and 671 nm). Reprinted with permission from ref. 93. Copyright (2012) American Chemical Society.

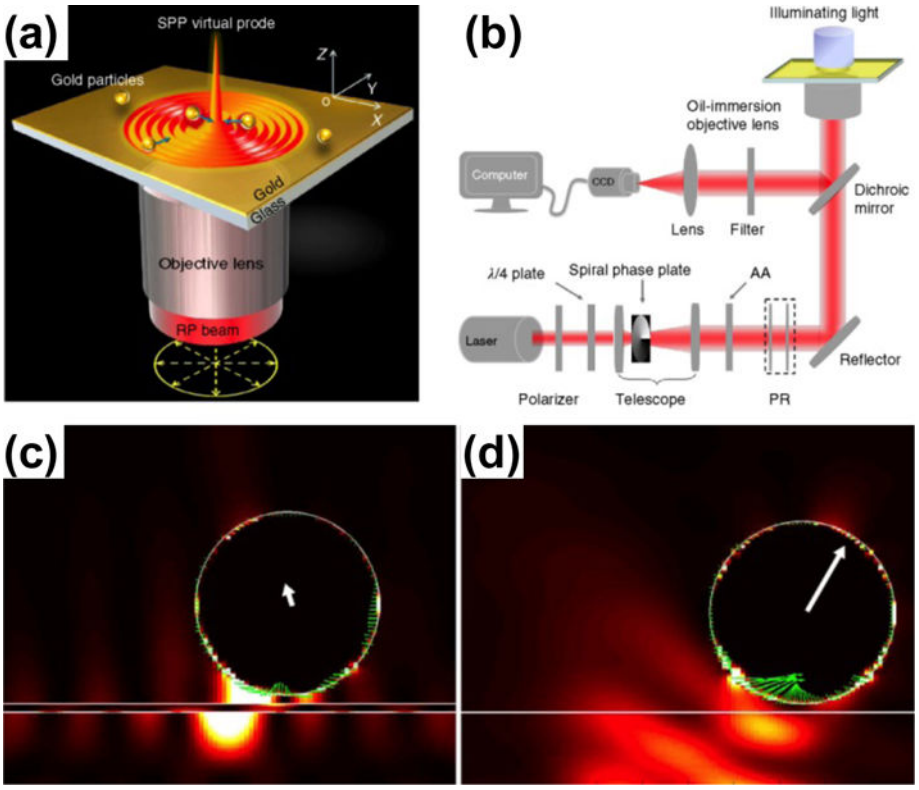

Figure 12.

(a) Schematic illustration of trapping metal particles by the highly focused SPP fields. (b) Schematics of the experimental setup for trapping and monitoring metal particles with the focused SPP fields. (c, d) Comparison of scattering forces exerted on a metal particle in (c) plasmonic tweezers and (d) optical tweezers. Reprinted with permission from ref. 94. Copyright (2013) Nature Publishing Group.

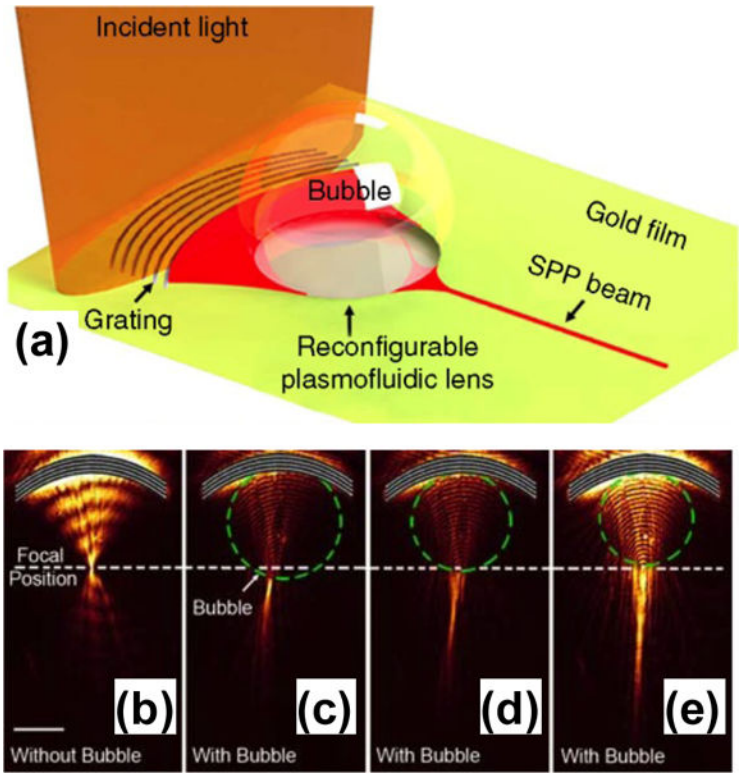

Figure 13.

(a) Schematic of the reconfigurable plasmofluidic lens. (b) Leakage radiation image of SPPs focused by an arc grating without surface bubble. (c)–(e) Leakage radiation image for SPPs propagating through three surface bubbles with different diameters. Reprinted with permission from ref. 36. Copyright (2013) Nature Publishing Group.

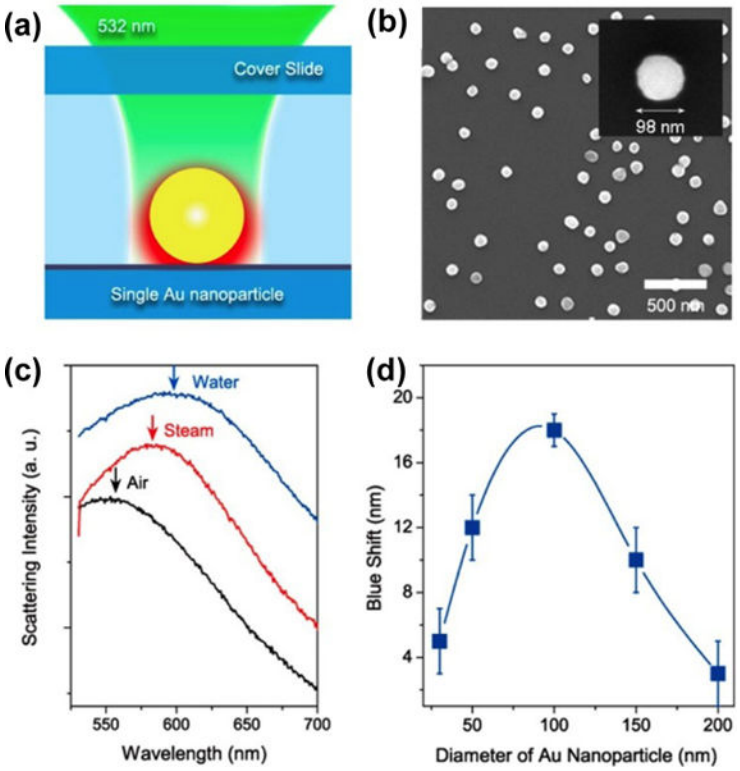

Figure 14.

(a) Schematic of illumination and heating of a single Au nanoparticle by a laser beam. (b) SEM image of Au nanoparticles on a glass substrate. (c) Scattering spectra of a 100 nm Au nanoparticle in air (black), water (blue), and an envelope of water vapor (red). (d) Correlation between the nanobubble-induced peak shift in LSPRs of Au nanoparticles and the particle diameter. Reprinted with permission from ref. 109. Copyright (2013) American Chemical Society.

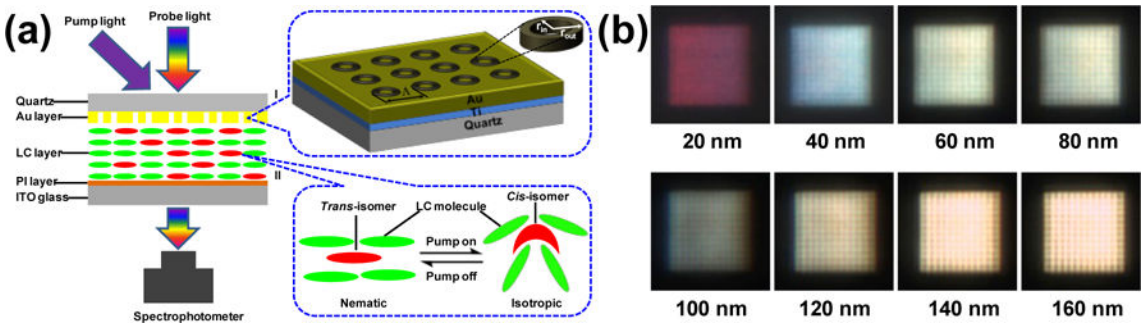

Figure 15.

(a) Schematic of light-driven plasmonic color filters based on photoresponsive liquid crystals. (b) Representative optical images of the color filters with different aperture sizes. Reprinted with permission from ref. 119. Copyright (2012) Wiley-VCH.

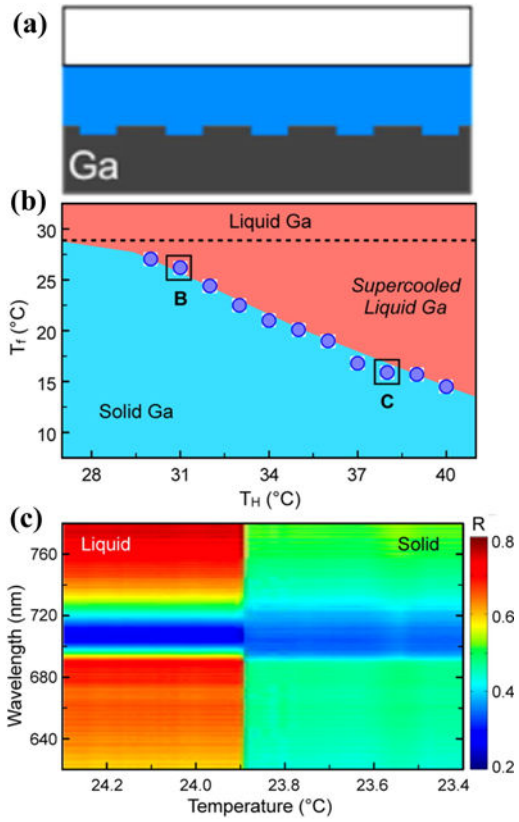

Figure 16.

(a) Cross-sectional view of a 1D Ga grating. (b) The liquid-solid phase transition of Ga with the effects of supercooling. T_f is the Ga freezing point and T_H is the initial holding temperature of the liquid phase. The dotted line corresponds to the melting point of 28.0 °C. (c) Real-time reflectance spectral map at T_H = 32.0 °C shows an abrupt change at 23.9 °C because of freezing of Ga. Reprinted with permission from ref. 122. Copyright (2012) American Chemical Society.

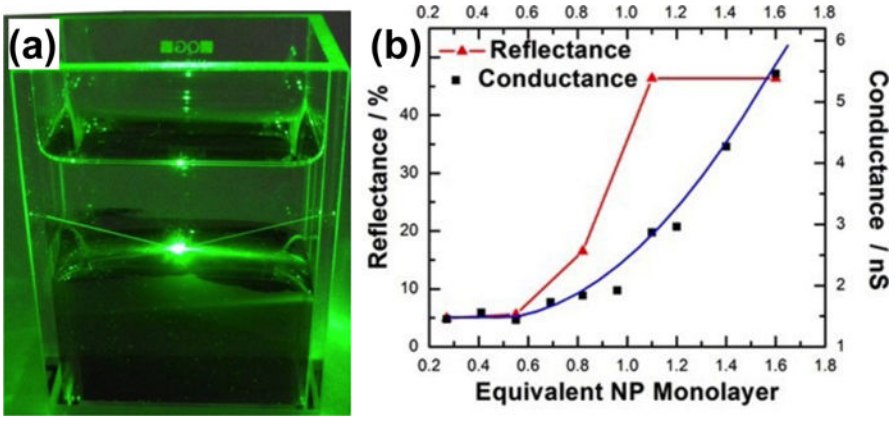

Figure 17.

(a) Optical image of a tunable mirror consisting of a monolayer of Au nanoparticles at the interfaces of two fluids illuminated with a green laser beam. The reflection and scattering of the beam by the monolayer are revealed. (b) The experimental reflectance and calculated electrical conductance as a function of the coverage of the monolayer of Au nanoparticles. Reprinted with permission from ref. 126. Copyright (2013) American Chemical Society.

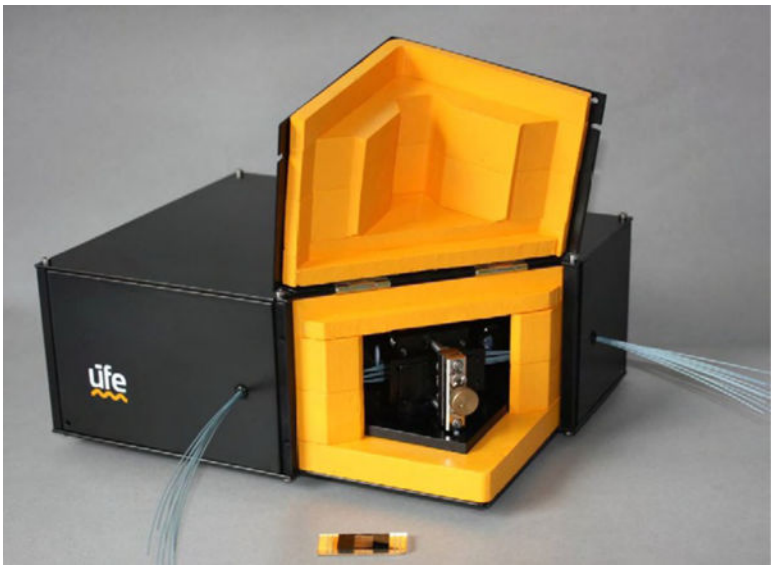

Figure 18.
Photograph of the prototype of a compact and multiplexed SPR sensor integrated with ten independent fluidic channels. Reprinted with permission from ref. 165. Copyright (2010) Elsevier.

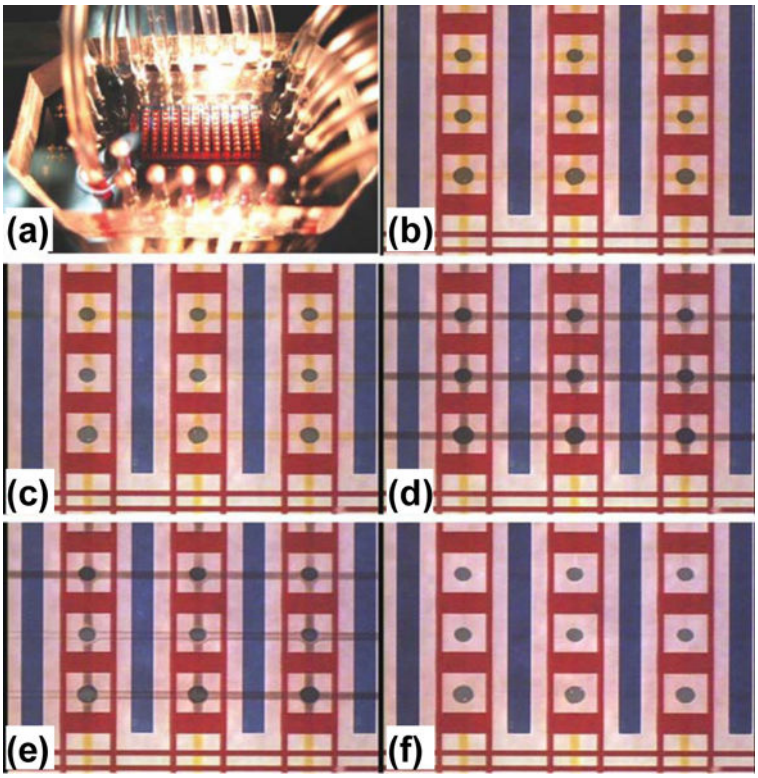

Figure 19.

(a) Photo of SPR imaging integrated with a microfluidic system. (b)–(f) Consecutive photos of the SPR imaging chip that is carrying out immunoreactions in the microfluidic system. (b) Vertical reagent injection step: a reagent (yellow liquid) is injected into the flow channels and then delivered to the Au spots. (c) First rinse step: a washing buffer (clear liquid) is injected to rinse the Au spots. (d) Horizontal reagent injection step: a reagent (black liquid) is injected into the flow channels then delivered to the Au spots. (e) Second rinse step: a washing buffer (clear liquid) is injected to rinse the Au spots. (f) The channels in the microfluidic device are clear after the second rinse. Reprinted with permission from ref. 168. Copyright (2008) Royal Society of Chemistry.

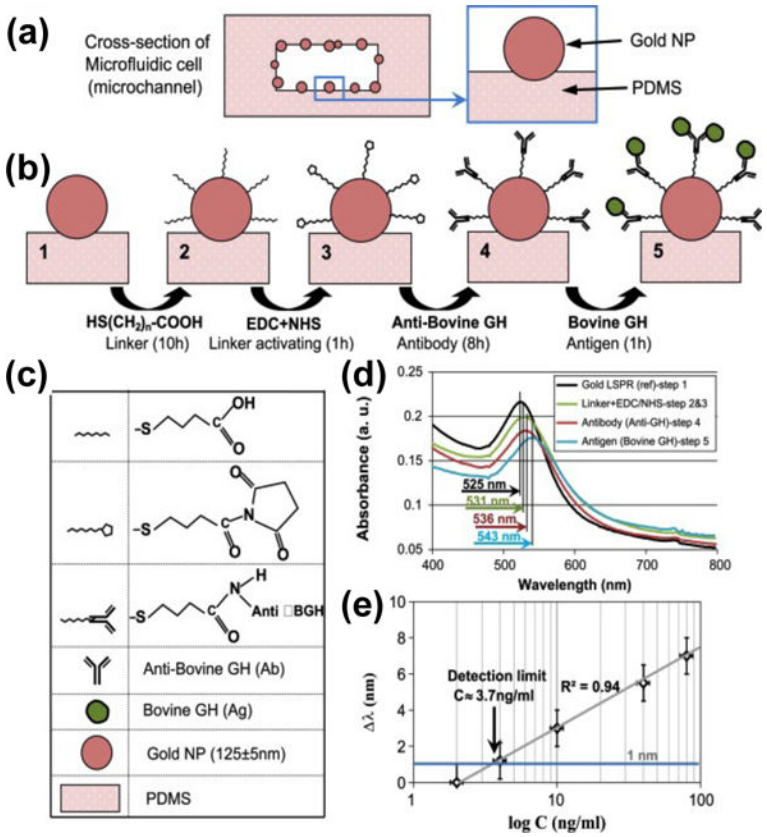

Figure 20.

An LSPR-microfluidic sensor based on metal nanoparticles immobilized on the sidewalls of microfluidic channels. (a) Cross-sectional view of a microfluidic channel with Au nanoparticles on the sidewalls. (b) Schematic illustration of the sensing protocol with legend shown in (c). (d) LSPR spectra of Au nanoparticles measured at four different stages. (e) Peak shift of LSPRs as a function of analyte concentration. Reprinted with permission from ref. 179. Copyright (2013) Elsevier.

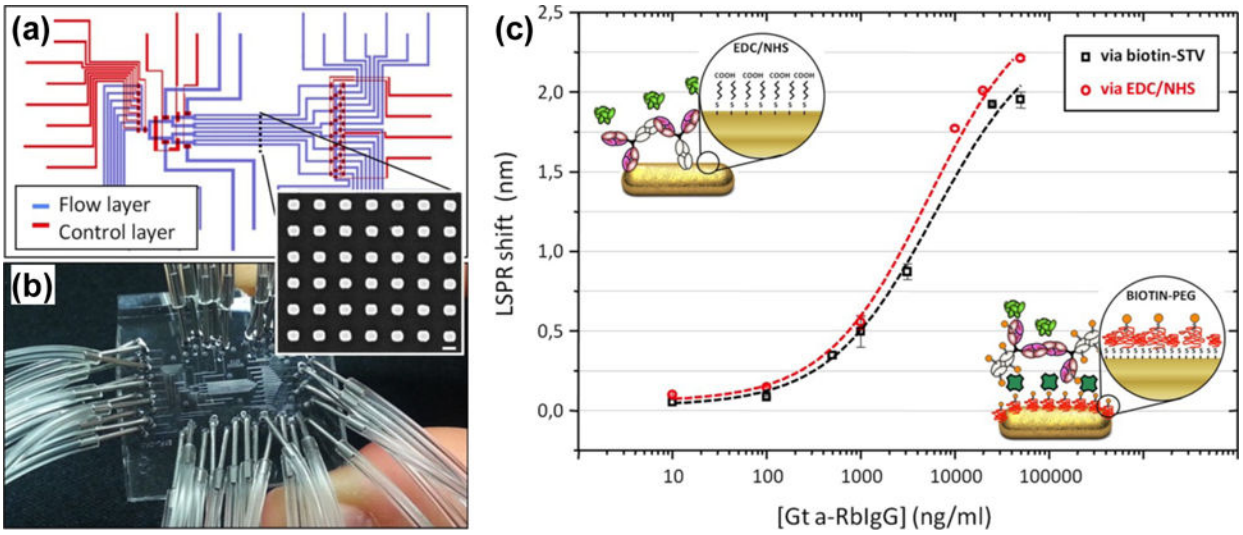

Figure 21.

(a) Schematic illustration of LSPR sensors consisted of multiple microfluidic channels on substrates immobilized with Au nanorod arrays. (b) Photo of the LSPR sensors chip. (c) Comparison of the performances of LSPR sensors, i.e., LSPR peak shit v.s. concentration of analytes, between two different receptors: unmodified receptor using the EDC/NHS approach and biotin conjugate of the same receptor. Reprinted with permission from ref. 183. Copyright (2014) American Chemical Society.

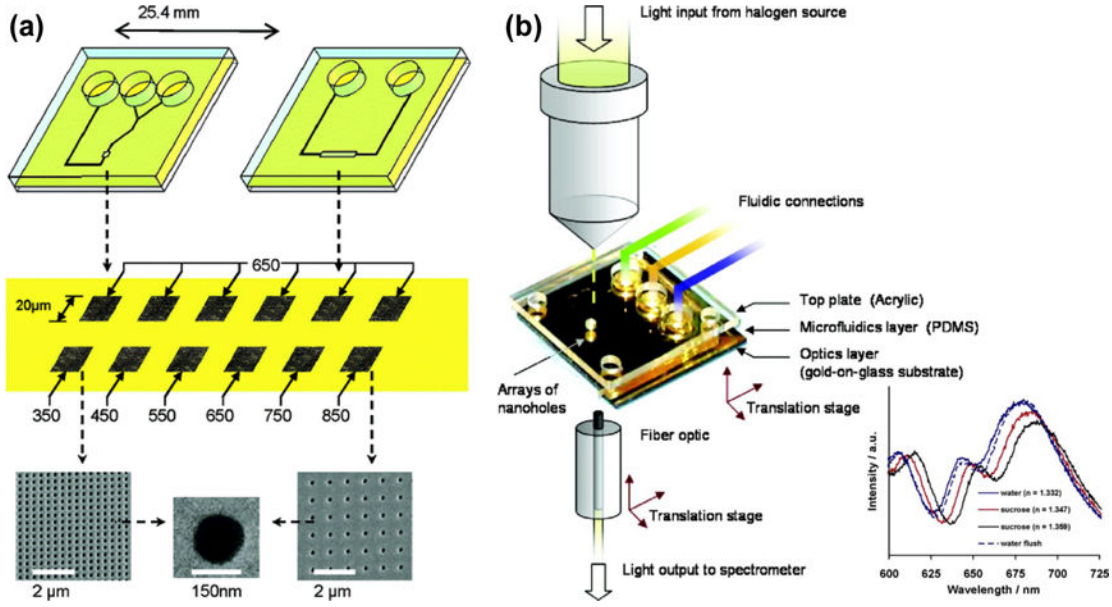

Figure 22.

(a) Schematic of plasmofluidic sensors that integrate microfluidic channels with EOT substrates. (b) Schematic of the experimental setup for detection applications. Inset shows the transmission EOT spectra for pure water and sucrose solutions with increasing refractive index. Reprinted with permission from ref. 189. Copyright (2007) American Chemical Society.

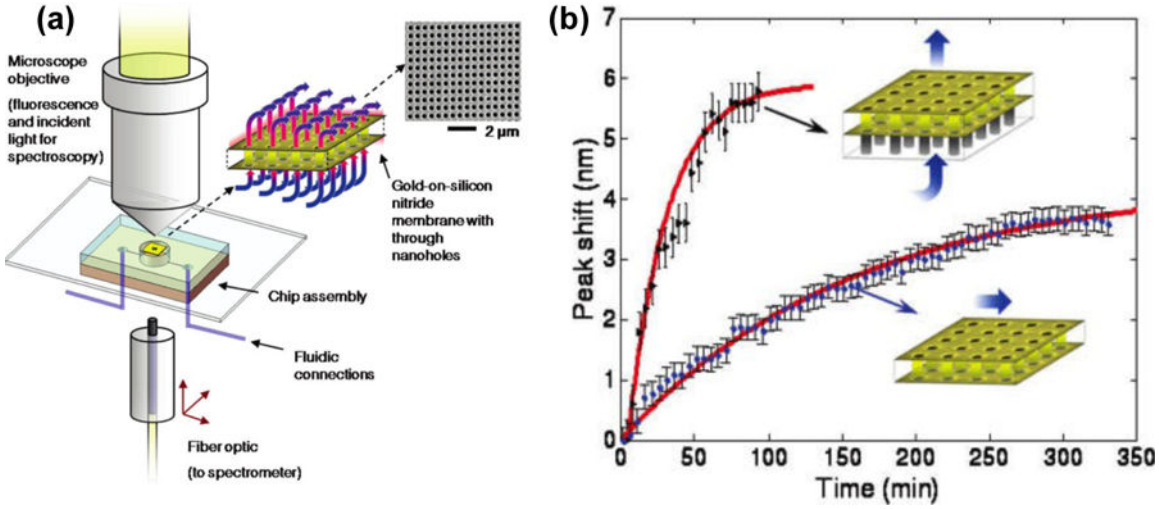

Figure 23.

(a) Schematic of the optical and fluidic test setup employed for both fluorescence and transmission spectroscopy based on the flow-through nanohole arrays. (b) Comparison of sensing performances with flow-over and flow-through formats as indicated in inset. Reprinted with permission from ref. 194. Copyright (2009) American Chemical Society.

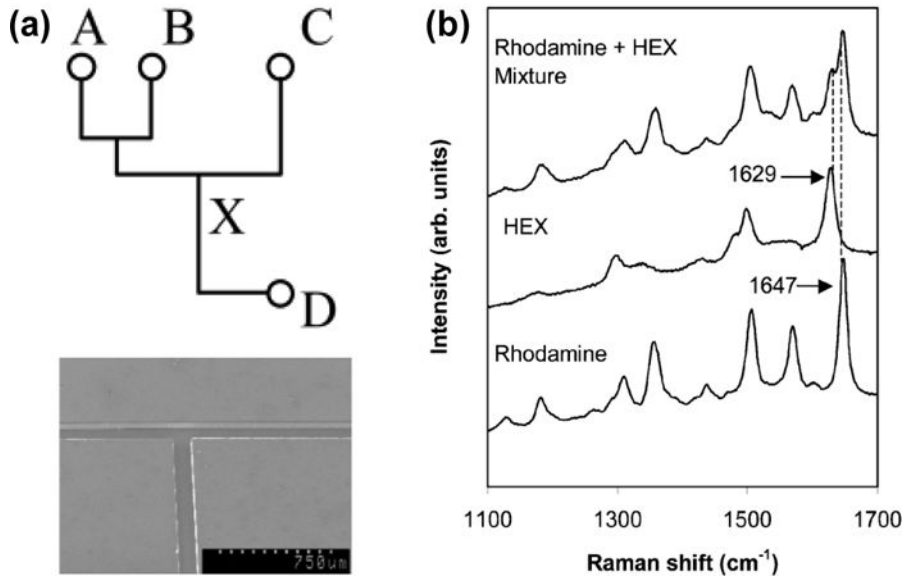

Figure 24.

(a) Schematic diagram of a SERS-microfluidic chip (upper) and SEM image of part of a PDMS microfluidic platform (below). (b) SERS spectra from rhodamine and HEX labeled oligonucleotides and from a mixture of both analytes. Reprinted with permission from ref. 206. Copyright (2004) Royal Society of Chemistry.

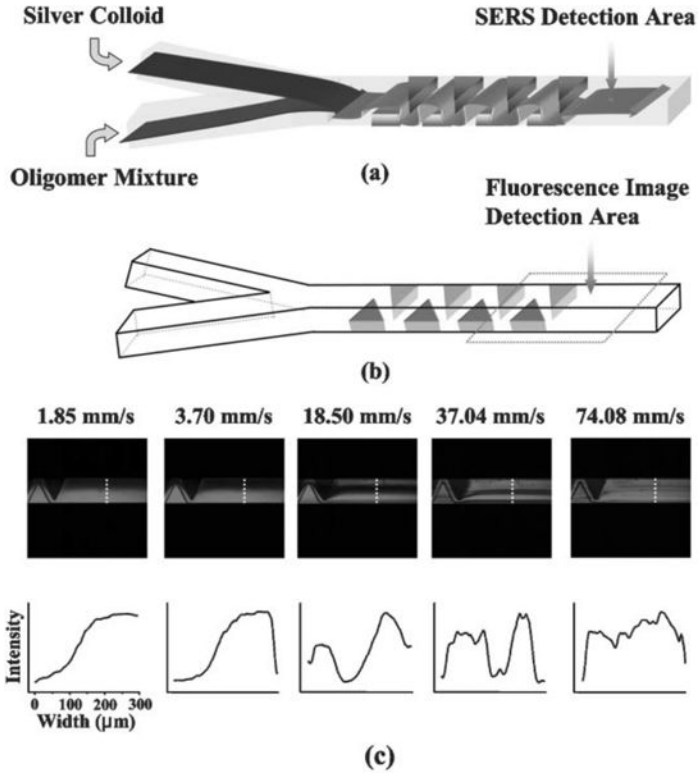

Figure 25.

(a) Schematic illustration of increased mixing of metal nanoparticles and analytes in a teeth-shaped microfluidic channel. (b) A detailed structure of the teeth-shaped microfluidic channel. (c) Confocal fluorescence images reveal that the higher flow velocity (indicated by number on the top of image) leads to the better mixing. Reprinted with permission from ref. 202. Copyright (2005) Royal Society of Chemistry.